

THE EFFECT OF HYPEROSMOLARITY ON FLUID-PHASE AND RECEPTOR-  
MEDIATED ENDOCYTOSIS IN P388D1 MACROPHAGES

Thesis presented by

MICHAEL JOHN BEGG

in fulfilment of the requirements for the degree of

MASTER OF SCIENCE

in

MEDICAL SCIENCES (MEDICAL BIOCHEMISTRY)

in the

FACULTY OF MEDICINE  
UNIVERSITY OF CAPE TOWN

SUPERVISOR: Associate Professor Lutz Thilo

December 1991

The University of Cape Town has been given  
the right to reproduce this thesis in whole  
or in part. Copyright is held by the author.

The copyright of this thesis vests in the author. No quotation from it or information derived from it is to be published without full acknowledgement of the source. The thesis is to be used for private study or non-commercial research purposes only.

Published by the University of Cape Town (UCT) in terms of the non-exclusive license granted to UCT by the author.

I, 

Signed by candidate
---------------------

 hereby declare that the work on which this thesis is based is original (except where acknowledgements indicate otherwise) and that neither the whole work nor any part of it has been, is being, or is to be submitted for another degree in this or any other University.

I empower the University to reproduce for the purpose of research either the whole or any portion of the contents in any manner whatsoever.

**ABSTRACT**

Extracellular components can be internalized by either receptor-mediated or fluid-phase endocytosis. Receptor-mediated endocytosis involves the internalization of receptor-ligand complexes into coated vesicles of about 0.1  $\mu\text{m}$  in diameter. The average diameter of primary pinocytic vesicles has been calculated to be 0.24 - 0.28  $\mu\text{m}$  (20). The discrepancy in size between coated vesicles and the average pinosome diameter can be explained if, in addition to coated vesicles, another endocytic process involving vesicles larger than 0.28  $\mu\text{m}$  in diameter takes place. These two vesicle types could together produce an average diameter of 0.24  $\mu\text{m}$ . This hypothesis suggests that coated vesicles cannot fully account for fluid-phase uptake. Hypertonic conditions can selectively inhibit receptor-mediated endocytosis, leaving fluid-phase uptake unaffected (34), again suggesting that an alternative to coated pit-mediated uptake exists.

In this study we determined the volume-weighted average diameter of primary pinocytic vesicles under hypertonic conditions (0.52 osm) where receptor-mediated uptake of transferrin was selectively inhibited by 42%. Fluid-phase uptake of FITC-dextran was unaffected by 0.52 osm medium. The internalization rate of  $^3\text{H}$ -galactose-labelled plasma membrane was reduced from 2.6 %/min to 1.5 %/min. The decrease in the rate of membrane internalization, without a reduction in the rate of fluid uptake at hypertonicity, implied a reduced surface to volume ratio of the pinocytic vesicles formed under these conditions. This suggested an increase in the average

diameter of primary pinocytic vesicles. Membrane internalization rates were calculated on the assumption that all labelled cell-surface constituents were internalized to the same relative extent, as has been shown previously for isotonic conditions. This assumption was also shown to hold true under isotonic conditions. The reduced rate of membrane internalization under hypertonic conditions was shown not to be due to the exclusion of any labelled protein species from internalized vesicles. The larger average vesicle size determined under conditions of selective reduction of coated vesicle formation (i.e hypertonicity), demonstrates the existence of a population of larger pinosomes involved in a possible alternative mechanism to coated-pit-mediated endocytosis.

ACNOWLEDGEMENTS

I would like to express my sincere thanks and appreciation to:

Assoc. Prof. Lutz Thilo, my supervisor, for his guidance, support and constructive criticism throughout this study.

Prof. Wieland Gevers, for providing the facilities and opportunities, without which this work would not have been possible.

Dr Tom Haylett, for his advice and practical know-how.

Stephen Fortuin, for his invaluable help and technical assistance.

Kerrin, for your unending love, support and encouragement, which helped me through those sleepless nights.

My family, for their moral support and understanding through some difficult times.

My friends and colleagues, especially Brent, Judy, Sharon, Ian, and Mike, for their advice and encouragement, both socially and academically.

The Medical Research Council, the Foundation for Research Development and the University of Cape Town for their financial assistance.

ABBREVIATIONS

ASOR	Asialo-orosmuroid receptor
ATP	Adenosine triphosphate
BSA	bovine serum albumin
°C	degrees centigrade
cpm	counts per minute
dpm	disintegrations per minute
EDTA	(ethylenediamine)-tetraacetic acid
EGF	Epidermal growth factor
FITC	fluorescein isothiocyanate
g	unit of gravity
HEPES	4-(2-hydroxyethyl)-1-piperazine-ethanesulphonic acid
HRP	horseradish peroxidase
Kd	equilibrium dissociation constant
kD	kilodaltons - unit of molecular mass
LDL	Low density lipoprotein
M	molar
Mr	relative molecular mass
osm	osmoles (moles per kilogram)
PAGE	polyacrylamide gel electrophoresis
S.E.M.	standard error of the mean
SDS	sodium dodecyl sulphate
$t_{1/2}$	half-life

CONTENTS

ABSTRACT . . . . .	ii
ACKNOWLEDGEMENTS . . . . .	iv
ABBREVIATIONS. . . . .	v
CONTENTS . . . . .	vi
LIST OF FIGURES. . . . .	viii
LIST OF TABLES . . . . .	viii
CHAPTER 1: INTRODUCTION. . . . .	1
Endocytosis . . . . .	1
Quantification of the endocytic pathway . . . . .	12
Proposed aim and approach of this study . . . . .	15
CHAPTER 2: METHODS . . . . .	17
Cells . . . . .	17
Pinocytic uptake. . . . .	17
Fluorescence assay for FITC-dextran . . . . .	18
HRP assay . . . . .	19
Cell surface labelling with UDP[6- <sup>3</sup> H]- or UDP[U- <sup>14</sup> C]-galactose . . . . .	20
Internalization of labelled membrane glycoconjugates. . . . .	21
Removal of label from the cell surface. . . . .	21
HRP binding assay . . . . .	22
Preparation of <sup>125</sup> I-transferrin . . . . .	23
Iron loading. . . . .	23
Determination of cell viability by trypan blue exclusion. . . . .	24
Membrane isolation. . . . .	24
SDS-polyacrylamide gel electrophoresis. . . . .	25

CHAPTER 3: ENDOCYTTIC UPTAKE UNDER ISOTONIC AND	
HYPERTONIC CONDITIONS. . . . .	26
RESULTS AND DISCUSSION. . . . .	26
Fluid-phase uptake of FITC-dextran and HRP. . . . .	26
Receptor-mediated uptake of HRP . . . . .	28
The effect of hyperosmolarity on fluid-phase and	
HRP receptor-mediated endocytosis. . . . .	31
The effect of sucrose-induced hyperosmolarity on	
HRP binding at the cell surface. . . . .	39
The effect of hypertonicity on transferrin receptor-	
mediated endocytosis . . . . .	42
 CHAPTER 4: INTERNALIZATION OF <sup>3</sup> H-GALACTOSE LABELLED	
PLASMA-MEMBRANE GLYCOCONJUGATES. . . . .	50
RESULTS AND DISCUSSION. . . . .	50
Membrane internalization under hypertonic conditions. . . . .	51
Molecular-weight distribution of surface-labelled	
glycoconjugates internalized under hypertonic	
conditions . . . . .	56
 CHAPTER 5: CONCLUSION. . . . .	62
 APPENDIX . . . . .	68
 REFERENCES . . . . .	70

LIST OF FIGURES

FIG. 1	Model of receptor-mediated endocytosis and uncoupling of receptor ligand complexes in the CURL	5
FIG. 2	Fluid-phase uptake of FITC-Dextran and HRP. . . .	27
FIG. 3	Concentration dependence of HRP pinocytosis . . .	29
FIG. 4	Adsorptive uptake of HRP. . . . .	30
FIG. 5	Effect of osmolarity on endocytic uptake. . . . .	33
FIG. 6	Reversibility of the hypertonic effect. . . . .	35
FIG. 7	HRP binding . . . . .	43
FIG. 8	Effect of osmolarity on transferrin uptake vs fluid-phase uptake. . . . .	47
FIG. 9	Effect of hypertonicity on membrane internalization. . . . .	52
FIG. 10	Kinetics of <sup>3</sup> H-galactose release from the cell surface under isotonic and hypertonic conditions. . . . .	57
FIG. 11	Molecular-weight profile of internalized labelled plasma-membrane glycoconjugates . . . . .	60

LIST OF TABLES

TABLE I:	Literature review of possible endocytosis inhibitors useful for selective inhibition of receptor-mediated endocytosis. . . . .	10
TABLE II:	The effect of increasing osmolarity on endocytosis (A summary of results) . . . . .	64

## CHAPTER 1

### INTRODUCTION

#### Endocytosis

Endocytosis is the term used to describe the invagination of the cell surface membrane (plasma membrane) to form internal membrane-bound vesicles, incorporating material from the extracellular environment.

Different functions are served by such a process including the internalization of molecules such as low density lipoprotein (LDL) (1), transferrin (2), asialoglycoproteins (3), growth factors (4) and hormones (5); the transcytosis of components across epithelia (6); and the uptake of toxins (7) and viruses (8).

There are two main mechanisms whereby components can enter the endocytic pathway:

1. Receptor-mediated endocytosis
2. Fluid-phase endocytosis.

#### 1. Receptor-mediated endocytosis:

Receptor-mediated endocytosis involves the high affinity adsorption of a specific extracellular component e.g. LDL, to a specific cell surface protein (receptor). This specific binding results in the concentration of the extracellular component onto the plasma membrane of the cell. The receptor and ligand cluster at morphologically distinct depressions on the cell surface called coated pits (9), so termed because of

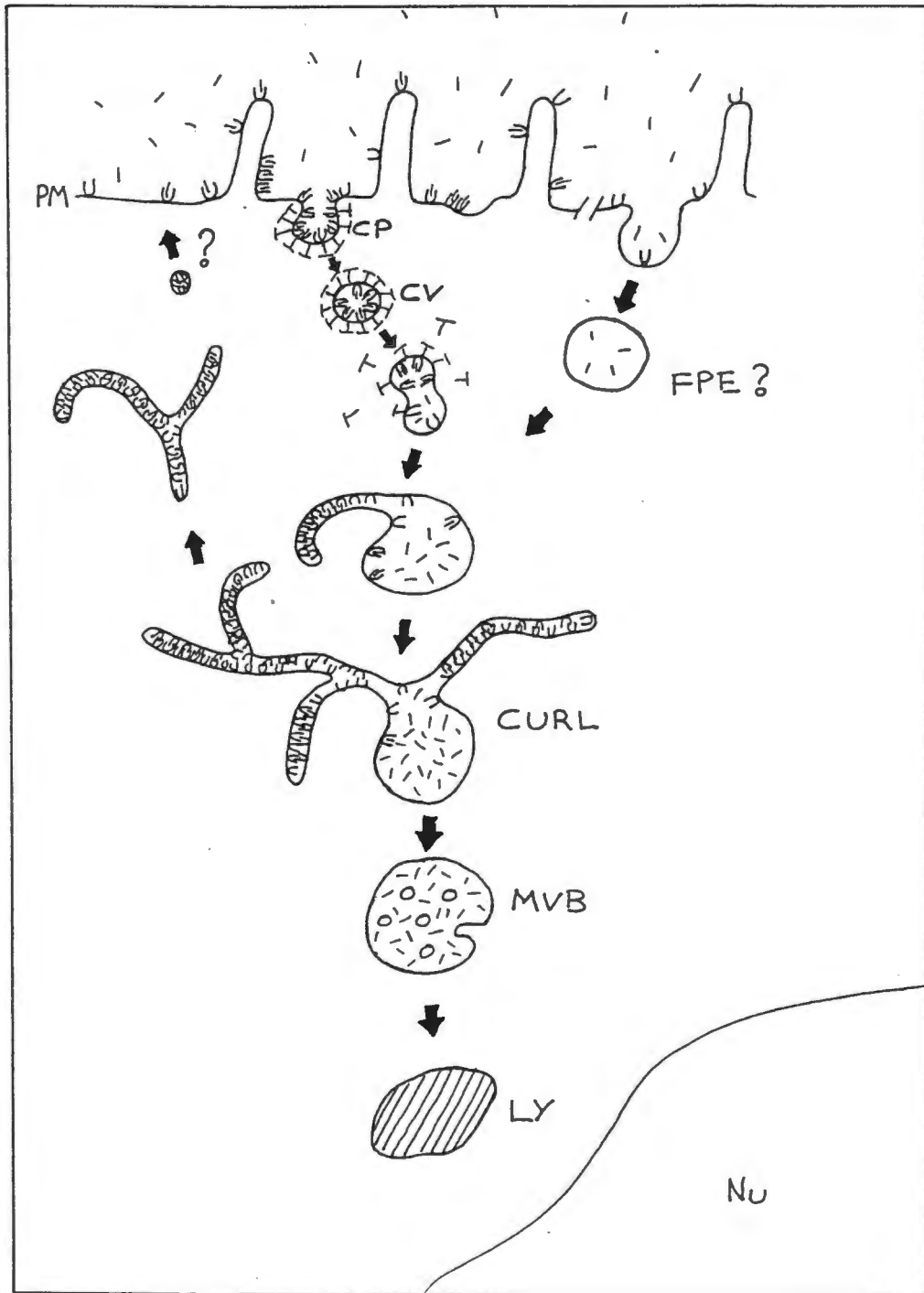
the presence of a bristle-like coat on the cytoplasmic surface of the depression. This coat is made up of a proteinaceous hexagonal lattice of clathrin monomers. It is this clathrin coat which acts as a molecular sieve and concentrates receptors to a level several hundred fold above that of the surrounding plasma membrane (10), presumably via interaction with the cytoplasmic tail of the receptor. Deletion of this portion of the transferrin receptor prevents the receptor from clustering at these sites (11), whereas insertion of a tyrosine in the cytoplasmic tail of influenza virus haemagglutinin allows this protein to cluster and to be internalized via coated pits (12).

After clustering of receptors in clathrin coated pits, the pits then invaginate and pinch off from the cell surface to form an intracellular clathrin coated vesicle. It has been estimated that as many as 3000 of these vesicles form per minute in an individual cell. The coated vesicles, containing high concentrations of receptors and receptor-ligand complexes, rapidly (< 1 min) lose their clathrin coat in an ATP-dependent manner (13). The resulting smooth vesicles then fuse with one another to form larger vesicles, which either mature into, or fuse with a pre-existing peripheral tubulovesicular compartment known as the CURL (Compartment for the Uncoupling of Receptor and Ligand) (3). This compartment is also known as the early endosomal compartment. There is much debate as to whether this is a pre-existing organelle or merely the product of multiple fusion events with smaller primary pinocytic vesicles. In addition to the fusion of primary vesicles with each other and finally with the early endosomal compartment, there is a

progressive acidification of the lumen of these vesicles via an ATP-dependent proton pump which is capable of acidifying the luminal pH to around pH 5.0 (14). This acidification of the lumen has been shown to be the chief mechanism for the dissociation of the receptor-ligand complex. The CURL compartment has been shown by double label (receptor vs ligand) immuno-electron microscopy, to be the site of dissociation of receptor-ligand complexes (3), and its tubulovesicular nature appears to be fundamental to the vectorial displacement of the receptor and ligand (15). The receptors have been found to be concentrated in the radiating tubules of the organelle, which were notably depleted of ligand. Conversely ligand accumulates in the vesicular portion of this compartment.

Geuze et al (16) found that asialoglycoprotein labelled with gold, entered the CURL tubules first before being delivered to the lumen of the CURL vesicles, giving some indication as to the site of entry into the CURL.

After the dissociation of the receptor-ligand complexes, the unoccupied receptors, now concentrated in the tubular elements of the CURL, are recycled to the plasma membrane for repeated internalization of ligand. In addition, the luminal contents of the CURL vesicular portion are routed into multivesicular bodies and finally to the lysosome for degradation or further processing (see Fig. 1).



(LEGEND ON FOLLOWING PAGE)

**FIG. 1. Model of receptor-mediated endocytosis and uncoupling of receptor ligand complexes in the CURL**

On the plasma membrane (PM), ligand (U) binds to receptors (1) which cluster in coated pits (CP) and internalize to form coated vesicles (CV). These coated vesicles rapidly lose their clathrin coats and fuse with one another to form larger vesicles. They then either fuse with, or develop into tubulo vesicular structures where ligand and receptors uncouple, hence the name CURL (Compartment for the Uncoupling of Receptor and Ligand). It is believed that receptors recycle via the tubular portions and ligand contained in the vesicular portions is delivered via multivesicular bodies (MVB) to lysosomes (LY) for degradation. A proposed alternative endocytic event involved in fluid uptake is also shown (FPE? - Fluid-phase endocytosis).

The average round trip time for a receptor (i.e. to be internalized and recycled) is 18 minutes (calculated from Table III (20)). This recycling of receptors enables the cell to internalize and unload 100 to 200 times more ligand than would be possible if only one cycle of endocytosis occurred, since the rate of synthesis of new receptors (30-60 hours for receptor turnover) is very much slower than the rate of internalization and recycling (18 minutes). Such recycling is however not characteristic of all receptors, resulting in the division of receptors into two broad classes or types.

Type 1: Constitutive receptor-mediated systems, where the receptor recycles through the endocytic pathway, regardless of the presence of ligand. These systems are usually involved with the uptake of metabolites such as LDL and transferrin (18,55).

Type 2: Ligand-induced internalization mechanisms, where recycling of the receptor is negligible, and most of the receptors are degraded along with their ligand in the lysosomes. These systems usually apply to signal bearing ligands such as epidermal growth factor (EGF) and other hormones. The lack of recycling is believed to act as a mechanism for down-regulation of the ligand-induced signal (19).

The CURL compartment appears to be the chief sorting station for internalized receptor-ligand complexes. This sorting includes the transfer of bulk fluid, dissociated ligand and

type 2 receptor-ligand complexes to the lysosome, while the majority of unoccupied receptors and internalized plasma membrane is recycled to the cell surface (20).

In the case of transferrin, the receptor and its ligand are taken up into the acidic endosomal compartment, where iron dissociates from the transferrin. Apotransferrin remains bound to the receptor and is recycled to the plasma-membrane where the apotransferrin dissociates from the receptor, allowing the binding and internalization of further diferric transferrin molecules (56-58).

Because transferrin does not dissociate from internalized receptors, maximal transferrin uptake is reached once all receptors are occupied within the endosomal compartment. Such saturation kinetics have been seen in a number of cell types, including Hep G2 cells (59), mouse teratocarcinoma cells (45), K562 cells (21) and human carcinoma A431 cells (56). Transferrin is thus an ideal marker for studies on the early endocytic pathway.

Weak bases and ionophores such as  $\text{NH}_4\text{Cl}$ , chloroquine, and monensin, prevent the acidification of the lumen of the endosomal compartment by dissipating the proton gradient. The lack of acidification prevents the receptor-ligand complexes from dissociating, which in turn disrupts recycling of receptors, hence undissociated receptor-ligand complexes appear to be trapped in swollen endosome-like compartments (21).

Monensin, however, did not interfere with recycling of bulk plasma membrane (22).

## 2. Fluid-phase endocytosis

This process, often known as constitutive pinocytosis, does not involve specific binding of ligand to cell-surface receptors but merely engulfs solute at the concentration as present in the extracellular medium. Solutes are internalized by simply entering the invagination at the cell surface, and subsequently being incorporated into the vesicle when it pinches off from the plasma membrane.

Fluid-phase endocytosis has been measured in a variety of cell types, using a variety of markers, such as Fluorescein-Isothiocyanate-dextran (FITC-dextran) (3,40,46),  $^3\text{H}$ -insulin (26),  $^{125}\text{I}$ -polyvinylpyrrolidone (27), horseradish peroxidase (HRP) (23),  $^{14}\text{C}$ -sucrose (7,25,27) and lucifer yellow (7,25), all of which fulfill the requirements of a typical fluid-phase marker. A fluid-phase marker is defined as "a readily soluble, membrane-impermeable, non-metabolised reagent, that does not modify cellular activities, has no binding affinity for the plasma-membrane and can be quantified with accuracy and high sensitivity at the level of single cells or cell populations" from ref. 40. HRP, however, has been shown to bind specifically to a mannose-fructose receptor on the plasma-membrane of macrophages (47,48). This renders it unsuitable for use as a fluid-phase marker in macrophages, but does make it a possible candidate as a receptor-mediated endocytic marker in these cells.

Fluid uptake has been shown to be non-linear in a number of cell types, including macrophages (28), fibroblasts (25), and hepatocytes (26). Such non-linearity may be due to constant exocytosis of accumulating marker (28). This retro-endocytosis causes a decrease in the rate of accumulation of fluid, until a new steady-state uptake rate is reached (i.e. initial rate - exocytosis rate = net uptake rate) (25,27,28). The degree of retro-endocytosis of pinocytosed fluid varies for different cell types. In some cells, fluid uptake has been linear (30), although in most studies, there has been at least some degree of non-linearity involved. Accumulated fluid is then delivered to the lysosomes for degradation, in the same manner as ligand internalized by receptor-mediated endocytosis.

Originally it was believed that all fluid uptake was due to fluid incorporated into coated vesicles as they pinched off from the plasma membrane. More recent work, however, has indicated that there may be multiple paths of endocytosis (34,35,61-63). Studies using specific inhibitors of the coated pit-mediated pathway, suggest that this pathway contributes only a minor portion to fluid uptake (51,52). Such selective inhibition has aroused interest in the possible role of an alternative uptake mechanism (see Table I).

TABLE I: Literature review of possible endocytosis inhibitors useful for selective inhibition of receptor-mediated endocytosis:

TREATMENT	COATED PIT INHIBITION	FLUID-PHASE INHIBITION	LIGAND	OSMOLARITY (OSMOLES)	CELL TYPE	REFERENCE
K <sup>+</sup> Depletion	YES	N/A	LDL/EGF	-	Fibroblast	66
Hypertonicity	YES	NO	f-nleleuphe	0.75	PMN Leucocytes	34
Hypertonicity	YES	N/A	ASOR	0.55	Hepatocytes	52,51
Hypertonicity	YES	YES	$\alpha_2$ Macroglobulin	0.60	3T3 L1 Fibroblasts	53
Hypertonicity	YES	YES	LDL	0.75	Fibroblasts	36
Extracellular Acidification	N/A	YES	HRP fluid-phase	-	BHK Celss	67
Cytosolic Acidification	YES	NO	Transferrin EGF.	-	Hep G2 Hela Sw Vera	35
Cytosolic Acidification	N/A	YES	HRP fluid-phase	-	Fibroblasts	37
Cytosolic Acidification	YES	YES	Transferrin	-	CCL 39 Cell line	65

N/A - Information not available

Daukas and Zigmond (34) have reported that in leucocytes hypertonic conditions selectively inhibit the receptor-mediated uptake of the chemotactic peptide N-formylnorleucylleucyl-phenylalanine, without affecting the fluid-phase uptake of  $^{14}\text{C}$ -sucrose. This selective inhibition by hyperosmolarity has been confirmed in hepatocytes using asialo-orosmuroid as a receptor-mediated marker and lucifer yellow as a fluid-phase label (51,52).

Acidification of the cytosol has been shown to have the same effect as hypertonicity, by inhibiting the receptor-mediated uptake of EGF and transferrin, without significantly affecting fluid-phase uptake of lucifer yellow or ricin (35).

Both the above systems have the same effect on clathrin coated pits, as they induce the formation of clathrin microcages, which remain stubbornly attached to the cytoplasmic surface of the plasma membrane and thereby prevent any uptake via this route (36,37).

Conversely, Sandvig and van Deurs (7) have demonstrated the selective modulation of fluid-phase uptake of ricin and lucifer yellow by cytoskeletal inhibitors such as cytochalasin D, without any alteration in transferrin endocytosis. This method however, results in only 50-60% inhibition of fluid-phase uptake but demonstrates the ability to selectively modulate one mode of uptake without significantly altering the other.

### Quantification of the endocytic pathways

The entire endosomal pathway is made up of a series of membrane bound compartments which interact with each other through uni- or bi-directional flow of both membrane and contents. Quantitative analyses deal with membrane pool sizes and membrane exchange rates between them.

### Morphological analysis

Morphometric analysis of the endocytic pathway has provided the majority of evidence for the size of, and kinetic relationships between, compartments of the endocytic pathway. Studies in macrophages using HRP as a luminal endocytic marker (24), have shown that both the volume and size of pinocytic vesicles increase over the first five minutes of internalization and subsequently reach a plateau. The increase in the size of the labelled vesicles suggests that, with time, small primary endocytic vesicles fuse to form larger vesicles.

The rate at which both HRP-labelled fluid and HRP-tagged membrane enter the cell has been found to be 10 times faster than the appearance in the lysosomes and suggests that excess membrane and fluid undergo retroendocytosis (24). Further analysis of the rates of HRP tagged membrane flow (cf. review 20), shows that the surface to volume ratio of HRP stained endosomes decreases from  $14 \mu\text{m}^2/\mu\text{m}^3$  of membrane at 0.5 minutes, to  $10 \mu\text{m}^2/\mu\text{m}^3$  at 5 minutes, after the addition of HRP to the extracellular medium. From the kinetics of this change, the size of primary pinocytic vesicles prior to pinosome-pinosome fusion has been calculated as  $0.28 \mu\text{m}$  (20).

Kinetic studies of fluid-phase endocytosis in rat hepatocytes (26) and alveolar macrophages (28), show two kinetically distinct compartments associated with this fluid uptake. 1) A rapidly filling compartment ( $t_{1/2}$  2-5 min), with a size of 2.5-3% of the cell volume, and 2) a larger compartment with a much slower turnover ( $t_{1/2}$  > 180 min). Analysis of uptake and recycling of the fluid-phase markers ( $^{125}\text{I}$  polyvinylpyrrolidone and  $^{14}\text{C}$ -sucrose in fibroblasts has similarly shown a small rapidly filling and recycling compartment, and a second larger, slower turnover compartment (25).

These two kinetic compartments are believed to be: the endosome compartment which is small and turns over with a half-life of about 5 minutes; and the lysosomal compartment which has a greater capacity and recycles at a much slower rate ( $t_{1/2}$  > 180 min).

#### Trafficking of labelled plasma membrane

Previously, all measurements of membrane areas associated with the intracellular endocytic compartments have been achieved by morphometric stereological analysis of membrane associated with endocytosed markers. Reversible labelling of cell-surface glycoconjugates with  $^3\text{H}$ -galactose has provided a general plasma-membrane marker for analysis of plasma-membrane redistribution into the endocytic pathway upon warming of the cells from  $0^\circ\text{C}$  to  $37^\circ\text{C}$  (32). This redistribution has been observed via the inaccessibility of  $^3\text{H}$ -galactose to removal by an extracellular administered enzyme,  $\beta$ -galactosidase, at  $0^\circ\text{C}$ .

Redistribution kinetics are biphasic, consisting of two exponential functions. These kinetics are explained in terms of membrane flow between the plasma membrane and two consecutive intracellular compartments. The relative sizes of the plasma-membrane, the first and second compartments, in terms of labelled plasma-membrane constituents, are 100 : 12.5 : 7.5, respectively. The two internal kinetic compartments have been suggested by the authors to be the same as those described by Steinman et al (24) using the fluid-phase marker HRP; i.e. the endosomal and lysosomal compartments, respectively.

The redistribution of label from the plasma membrane into the first compartment is extremely rapid, corresponding to a membrane internalization rate of 4.7% of the plasma-membrane per minute. This results in the compartment being filled with incoming membrane every 2.7 minutes, and thus suggests a rapid recycling of plasma membrane from this first compartment.

By comparing the initial rates of both membrane internalization and of concomitant volume uptake, a surface to volume ratio for primary pinocytic vesicles of  $52.8 \mu\text{m}^3/1300 \mu\text{m}^2$  is obtained. Assuming a spherical nature of these primary pinosomes, a volume weighted average diameter (rather than weighted to relative abundance) ( $6 \times \text{volume} / \text{surface area}$ ) of  $0.24 \mu\text{m}$  has been calculated. This compares very well with a value of  $0.28 \mu\text{m}$  as obtained by morphometric techniques for a number of different cell types (review Table I in 20).

Both morphometric and kinetic analysis (24,32) of primary pinosome size suggest a volume-weighted average diameter of 0.24 - 0.28  $\mu\text{m}$ . Coated pit-mediated uptake yields coated vesicles of an average size of 0.1  $\mu\text{m}$  (33). This suggests that the small coated vesicles are not the only contributors to fluid-phase uptake, implying a population of larger primary pinosomes which are not associated with coated pit-mediated uptake.

#### Proposed aim and approach of this study

The main aim of this project was to characterise a population of non-coated primary pinosomes as the major or additional contributors to fluid-phase uptake. The approach was then to inhibit coated pit-mediated uptake (i.e. coated vesicle formation), and to determine the volume-weighted average diameter of the primary pinosome under these conditions.

Hypertonic conditions were chosen as the mode of inhibition of receptor-mediated uptake, since complications are minimised and maintenance of the conditions can be sustained over sufficiently long periods. Cytosolic acidification, on the other hand, involves the accurate determination of the manipulated internal pH for each experiment, and this is prone to considerable variation during the time course of the experiment (35).

The volume-weighted average diameter (0.24  $\mu\text{m}$ ) is the calculated average size of all vesicles involved in uptake. Selectively eliminating the contribution of the small coated

vesicles ( $0.1\mu\text{m}$ ) to the average size, by hypertonicity, should shift the average to a greater size than that calculated for isotonic conditions. This shift in average size will be dependent on the relative numbers of coated vesicles, and therefore their contributions to both fluid uptake and membrane internalization.

## CHAPTER 2

### METHODS

#### Cells

A mouse tumour cell-line P388D1, classified as having numerous macrophage-like characteristics (38,39) was cultivated in RPMI 1640 medium, supplemented with 10% foetal calf serum, penicillin at 100 IU/ml and streptomycin at 100 µg/ml, in a 5% CO<sub>2</sub> environment at 37°C. Cells were propagated into suspension from monolayer cultures in 175 cm<sup>2</sup> tissue culture flasks (Falcon, Beckton-Dickinson, New Jersey) with 35 ml of medium per flask. The medium was replaced every 24 hours.

The cells were harvested not later than 24 hours after application of fresh medium. The cell-containing medium was centrifuged at 150 x g for 5 min at 4°C. The cell pellet was then washed three times with 30 ml of ice-cold HeRPMI (RPMI 1640, 10 mM HEPES, pH 7.4). A growth period of 24 hours resulted in about 10 x 10<sup>6</sup> suspended cells per flask.

#### Pinocytotic uptake

Pinocytosis was performed as described by Oliver et al (40). Cells were harvested and washed three times in ice-cold HeRPMI. They were then resuspended in HeRPMI at 5 x 10<sup>6</sup> cells/ml and warmed to 37°C in suspension for 15 minutes to allow full recovery after cold treatment. At time zero, FITC-Dextran (40 kD Sigma Chemical Co., St Louis, MO) (concentrations adjusted for each experiment, see legend) and/or HRP (Type II, Sigma Chemical Co, St Louis, MO) dissolved in HeRPMI (10% of final

volume), was added and mixed into the cell suspension at 37°C. At various times, samples ( $2.5 \times 10^6$  cells) were removed and immediately placed into 3 ml ice-cold HeS (10 mM Hepes, 150 mM NaCl, pH 7.4), to stop further pinocytosis. Bulk external marker was then removed as follows: The cells were pelleted by centrifugation at 150 x g for 5 min, the supernatants aspirated and the cells resuspended in 3 ml ice-cold HeS. This procedure was repeated three times, whereafter the cells were transferred to new tubes and pelleted as before. These cell pellets were then resuspended in 1 ml HeS. The transfer to new tubes resulted in a substantial reduction of background caused by marker binding to the sides of the tubes.

The cell number in each sample was determined by removing 100  $\mu$ l of cell suspension and counting it in a Coulter counter (Coulter Electronics, Florida). The remaining cells were then lysed in 0.1% Triton X100, by adding 100  $\mu$ l of 1% Triton X100, to release internalized marker.

The bulk of the cell debris was removed by centrifugation at 1000 x g for 20 min, and the concentration of FITC-Dextran and/or HRP in the supernatants was measured and related to the cell concentration in each sample.

#### Fluorescence assay for FITC-Dextran

To convert fluorescence intensity/cell to volume/cell, a series of standard samples was prepared by taking 10  $\mu$ l of the uptake medium, including marker, and diluting this 100 times into 1 ml of HeS. From this dilution, 10, 20, 30 and 40  $\mu$ l was removed

and each placed in 1 ml of HeS resulting in a standard curve representing 100, 200, 300 and 400 nl of original solution respectively. This procedure was chosen because it resulted in a fluorescence signal in the same order of magnitude as that obtained via cellular uptake. Both the cell and standard samples were then measured for fluorescence in a fluorescence spectrometer (Perkin-Elmer LS-5) at 470 nm excitation and 520 nm emission. Standard curves were linear and the value of the slope (fluorescence intensity (FI) / nl) was used to convert the sample value (FI/10<sup>6</sup> cells) to nl/10<sup>6</sup> cells (i.e.  $\mu\text{m}^3/\text{cell}$ ).

#### HRP assay

The HRP assay was performed as previously described (41). The substrate solution was made up by titrating Solution A (20 mM Na<sub>2</sub>HPO<sub>4</sub>, 110 mM NaCl) with solution B (20 mM citric acid, 150 mM NaCl) to pH 4.3. To this, 0.55 mg/ml ABTS (Boehringer Mannheim) and 0.003% H<sub>2</sub>O<sub>2</sub>, was added. Standard samples were prepared as for FITC-Dextran, with the exception that for low concentrations of HRP (i.e. <30  $\mu\text{g}/\text{ml}$ ) a dilution of 1/10 as opposed to 1/100 was made. 50  $\mu\text{l}$  of solution was removed from all samples, including the standards, and placed in a 5 ml plastic tube.

0.5 ml of the substrate solution was added to each 50  $\mu\text{l}$  sample and this was then incubated at room temperature for 10-15 minutes. The reaction was stopped by adding 0.5 ml of stopping solution (100 mM Citric acid, 0.01 % NaN<sub>3</sub>). The absorbance was then measured at 420 nm and compared to that of the standard

curve to determine the amount of cell-associated HRP (ng/10<sup>6</sup> cells).

#### Cell surface labelling with UDP[6-<sup>3</sup>H]-or [U-<sup>14</sup>C]-galactose

Cell-surface labelling with UDP[6-<sup>3</sup>H]galactose or UDP[U-<sup>14</sup>C]galactose is based on the enzymatic linkage of UDP-galactose to terminal N-acetylglucosamine residues on cell-surface glycoconjugates by the enzyme galactosyltransferase (42).

All steps were performed on ice to prevent membrane internalization. Cells were harvested, washed, and resuspended at about 10<sup>8</sup> cells/ml in HeS. A reaction mixture was made as follows: 50  $\mu$ l (50 mM MnCl<sub>2</sub>), 50  $\mu$ l galactosyltransferase (0.25 units, Sigma Chemical Co., St Louis, MO) and 20  $\mu$ l UDP[6-<sup>3</sup>H]galactose (ammonium salt, 20 Ci/mmol, Amersham) or 100  $\mu$ l UDP[U-<sup>14</sup>C] galactose (lithium salt, 320 mCi/mmol, Amersham) was added to an Eppendorf tube. The volume was then made up to 220  $\mu$ l with HeS (The volumes used were adjusted in proportion to the number of cells to be labelled). This was then added at 0°C to a cell pellet of about 50 x 10<sup>6</sup> cells and the cells resuspended. The final suspension contained 5 mM MnCl<sub>2</sub>, galactosyltransferase ((0.5 Units/ml) and UDP[6-<sup>3</sup>H]galactose (2  $\mu$ M) or UDP[U-<sup>14</sup>C]-galactose (8  $\mu$ M). They were then incubated on ice for 30 minutes with periodic light agitation to resuspend the cells, and the reaction was stopped by a 1:10 dilution with HeS at 0°C. The cell pellet was then washed three times in 10 ml ice-cold HeS by centrifuging at 150 x g for 5 min.

### Internalization of labelled membrane glycoconjugates

UDP[6-<sup>3</sup>H]Galactose-labelled cells were resuspended at  $5 \times 10^6$  cells/ml in HeRPMI at 0°C. The cells were then rapidly warmed to 37°C in an orbital shaking waterbath. Triplicate samples of 0.5 ml, containing  $2.5 \times 10^6$  cells each, were removed at each time point, either into ice-cold HeS, or fixed rapidly in 2% glutaraldehyde (TAAB, England) and vortexed immediately. Samples for the zero time points were removed and fixed prior to warming to 37°C to prevent any internalization taking place. The samples were washed once in HeRPMI to block remaining glutaraldehyde, followed by a wash in HeS.

### Removal of label from the cell surface

Labelled cells, either fixed or non-fixed ( $2 \times 10^6$  cells/sample) were then resuspended at  $10^8$  cells/ml in HeS containing 0.2 units/ml  $\beta$ -galactosidase (*Streptococcus pneumoniae*), and incubated either for 30 minutes at 0°C for unfixed cells, or overnight at room temperature for glutaraldehyde-fixed cells. The reaction was stopped by diluting the reaction mixture five fold with HeS. The release of label was determined by removing equal-volumed samples of both the cell suspension and cell-free supernatant from each time-point sample. These were then placed on combustion pads (Packard) and separated as  $^3\text{H}_2\text{O}$  and  $^{14}\text{CO}_2$  by a sample oxidizer (model 306, Packard Instrument Co.), to be measured by scintillation counting (Tri-Carb 1900CA Liquid scintillation analyzer, Packard Instrument Co., Meriden,

CT.). The percent of released label was determined as follows:  
supernatant dpm/cell suspension dpm x 100 = % of label removed.(32)

#### HRP binding assay

Cells were resuspended at  $10^7$  cells/ml in HeRPMI. Samples of about 2 ml of the cell suspension were incubated for 20 min at 37°C. A small volume of HRP stock solution (4 mg/ml) was added with or without yeast mannan (2 mg/ml final concentration) (Sigma Chemical Co., St Louis, MO) (which competes for receptor binding) to the cells, to give the desired HRP concentration. The cells were incubated for 5 minutes at 37°C to effect binding, with a small degree of uptake. During this time a small fraction from each of the incubation mixtures, normally about 100  $\mu$ l, was removed for calibration of the HRP concentration. The cell suspensions, of about 2 ml, were then added to 8 ml of ice-cold HeSCa (HeS, 2 mM CaCl, 1 mM MgCl). All further steps were performed at 0°C. The cells were washed three times with 8 ml HeSCa, by centrifuging at 150 x g for 5 min and resuspending the cell pellet in HeSCa. Three 2.5 ml samples were then removed from the third wash. The remaining 0.5 ml were used to determine cell number, using a Coulter counter. Triplicate samples were centrifuged at 150 x g for 5 min and the supernatants were aspirated. The pellets were then acid washed by resuspending them in 1 ml (0.2 M NaAcetate, 0.5 M NaCl, pH 3.8) for 5 minutes (43). The cells were sedimented at 150 x g for 5 min and a 0.5 ml sample of the supernatant was removed. An aliquot of 100  $\mu$ l of this supernatant was used to measure HRP as previously described, and the number of HRP molecules associated with the cell surface was calculated.

### Preparation of $^{125}\text{I}$ -transferrin

Mouse transferrin (essentially iron-free (Sigma Chemical Co., St Louis, MO)) was iodinated by the Iodogen method of Fraker and Speck (44).

Glass kimble tubes were prepared by placing 100  $\mu\text{l}$  of chloroform (containing 0.5  $\mu\text{g}/\text{ml}$  iodogen, Pierce Chemical Co.) into tubes and evaporating this under nitrogen to coat the tubes with iodogen.  $\text{Na}^{125}\text{I}$  (2  $\mu\text{l}$  at 100  $\text{mCi}/\text{ml}$ ) was combined with 500  $\mu\text{l}$  of mouse transferrin (200  $\mu\text{g}/\text{ml}$ ) in an eppendorf tube. This solution was then placed in an iodogen tube on ice for five minutes to effect labelling of the transferrin with  $^{125}\text{I}$ . The reaction was stopped by removing the liquid with a pasteur pipette and sealing it in dialysis tubing (Spectra/por, MW cutoff 12-14 kD, diameter 10 mm, Spectrum Medical Industries, Los Angeles, California). The dialysis tubing was floated in 500 ml of cold saline EDTA (150 mM NaCl, 1 mM EDTA) which was changed every hour for the first three hours, and finally left in 1000 ml cold saline EDTA overnight. The specific activity was determined by relating the amount of  $^{125}\text{I}$ -label to protein as assayed using the technique of Lowry et al (68). Specific activities of  $1-2 \times 10^5$   $\text{cpm}/\mu\text{g}$  were obtained.

### Iron loading of transferrin

Iron loading of apotransferrin to form diferric transferrin was performed as adapted from Karin and Mintz (45). After iodination and dialysis, the dialysis tubing containing the

$^{125}\text{I}$ -transferrin was placed in 500 ml iron loading buffer (1 mg/ml  $\text{FeNH}_4$  citrate, in 10 mM  $\text{H}_2\text{S}$ , 10 mM  $\text{NaHCO}_3$ ) for 6 hrs, for diffusion of the iron loading solution into the dialysis membrane. The transferrin was then stored at  $-17^\circ\text{C}$ . Unlabelled transferrin was loaded with iron in the same manner.

#### Determination of cell viability by trypan blue exclusion

This assay is based on the exclusion of a dye, trypan blue, by viable cells. The procedure was performed as follows. 50  $\mu\text{l}$  of cell suspension was combined with 50  $\mu\text{l}$  of trypan blue stock solution (0.5% trypan blue (Merck), 140 mM  $\text{NaCl}$ , 4.7 mM  $\text{KCl}$ , 1.2 mM  $\text{KH}_2\text{PO}_4$ , 0.6 mM  $\text{MgSO}_4$ , 10 mM HEPES, pH 7.2). After 5 minutes at room temperature, a small sample was placed in a haemocytometer and viewed under a microscope. Viability was determined as the percentage of unstained cells relative to the total number of cells. Experiments were aborted if the cell viability was less than 85% after the experimental manipulation.

#### Membrane isolation

$^3\text{H}$ -galactose or  $^{14}\text{C}$ -galactose-labelled cells were resuspended in homogenization buffer (10 mM Tris-HCl pH 7.6, 1 mM EDTA, 0.25 M sucrose, and proteinase inhibitors: 1 mM Phenylmethylsulphonyl fluoride (PMSF) and 12.5  $\mu\text{M}$  leupeptin), at a concentration of not more than  $10^7$  cells/ml, and disrupted by sonication (30 x 1 second pulses, while kept on ice). A post-nuclear supernatant (PNS) was formed by pelleting the nuclei at  $750 \times g$  x 10 min. The PNS (about 10 ml) was then centrifuged at  $10^5 g$  for 60 min in a Beckman type 70 Ti rotor.

The membrane pellet was resuspended in about 100  $\mu$ l HeS, and solubilized for SDS-PAGE by mixing with an equal volume of 2 x sample buffer (20% glycerol V/V, 5% SDS, 0.1 M  $\beta$ -mercaptoethanol, 0.1% bromophenol blue) and heating to 90°C for 3 minutes.(41)

#### SDS Polyacrylamide gel electrophoresis

This was carried out in gradient slab gels (250 x 180 x 1.5 mm) 5-13% polyacrylamide and 0.1% SDS with a discontinuous buffer system. Electrophoresis was performed at 15 mA for about 15 hours. Standard molecular weight markers (SDS-200 and SDS70L, Sigma Chemical Co., St Louis, MO) were used for calibration. The protein bands were stained with coomassie brilliant blue (Sigma). The gel was dried and each lane was cut into about 100, 2.5 mm slices, which were then converted to  $^3\text{H}_2\text{O}$  and  $^{14}\text{CO}_2$  in a sample oxidizer for full separation of the isotopes, before determining radioactivity by Scintillation counting.(41)

### CHAPTER 3

#### ENDOCYTOSIS UNDER ISOTONIC AND HYPERTONIC CONDITIONS

##### RESULTS AND DISCUSSION

Determining relationships between receptor-mediated and fluid-phase endocytosis requires quantitation of these two processes individually. Specific markers can be used to distinguish between the two events. FITC-dextran was used as a fluid-phase marker while HRP and transferrin were used as receptor-mediated endocytic markers. Selective inhibition of receptor-mediated endocytosis by increased osmolarity was investigated.

##### Fluid-phase uptake of FITC-dextran vs HRP

FITC-dextran was used as a marker to measure fluid-phase endocytic uptake. Uptake was linear over sixty minutes indicating that subsequent retroendocytosis of marker was insignificant (Fig. 2). The rate of uptake ( $3.75 \mu\text{m}^3/\text{cell}/\text{min}$ ) as determined by linear regression was comparable to the rate obtained previously for this cell type ( $2.5 \mu\text{m}^3/\text{cell}/\text{min}$  (32)). The zero time value of about  $17 \mu\text{m}^3/\text{cell}$  was due to a combination of autofluorescence of the cell and light scattering. Cells incubated in the absence of FITC-dextran gave the same background value (data not shown).

To determine whether HRP could be used as a fluid-phase marker in P388D1 macrophages, cells were incubated at  $37^\circ\text{C}$  with a high concentration of HRP (0.5 mg/ml), in the presence of FITC-dextran as a control for fluid-phase uptake (Fig. 2). HRP was taken up in a very similar fashion to FITC-dextran, but with a

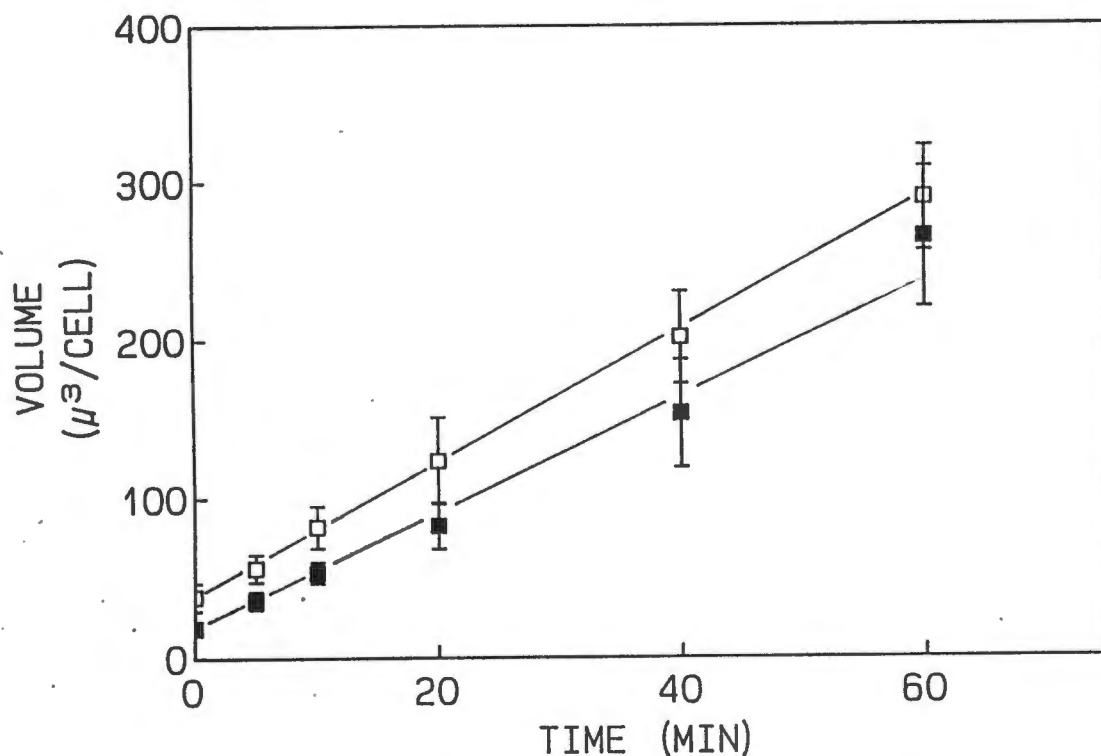


**FIG. 2. Fluid-phase uptake of FITC-Dextran and HRP**

Cells were equilibrated in HeRPMI for 15 min at 37°C. At time zero FITC-dextran (3 mg/ml) (■) and HRP (500  $\mu$ g/ml) (□) was added. At the indicated time points, 0.5 ml of cell suspension was removed and washed as described in METHODS. Cell associated FITC-Dextran and HRP was measured and the corresponding volume of endocytosed fluid was calculated. Data points are the average of 5 experiments with error bars (calculated formally as the S.E.M.) indicating the degree of systematic variation\* between individual experiments. The slopes indicate uptake rates of 3.75 and 4.17  $\mu\text{m}^3$ /cell/min, as measured for FITC-dextran and HRP respectively.

(\* Values at all time points for a given experiment were either lower or higher than the corresponding points in another experiment.)

10% higher rate ( $4.17 \mu\text{m}^3/\text{cell}/\text{min}$ ). Quantitatively this increase in rate would be consistent with a contribution by receptor-mediated uptake of HRP, possibly via the mannose receptor (cf. below). It could however also be due to uptake of HRP non-specifically bound to the cell surface.

#### Receptor-mediated uptake of HRP

Fluid-phase uptake, by definition, is linear with respect to concentration of the marker, whereas receptor-mediated uptake is non-linear, with a disproportionately higher rate of uptake at low ligand concentrations (i.e. below the  $K_d$ ), above which the increase in rate with increasing ligand concentrations will become less until a linear increase is reached, due to an increasing contribution by fluid-phase uptake.

Cells were incubated at  $37^\circ\text{C}$  with HRP at various concentrations, in the presence or absence of high concentrations (2 mg/ml) of yeast mannan, which can be used to compete for binding to the mannose-fucose receptor (47-49) (Fig. 3). The non-linearity dependence of the HRP uptake rate on HRP concentration was seen in the absence of yeast mannan. The disproportionately higher uptake rate at concentrations below 25  $\mu\text{g}/\text{ml}$  is indicative of a saturable binding of the ligand to the cell surface. The presence of excess mannan abolished any enhanced uptake of HRP at low concentrations, resulting in a completely linear relationship between concentration and uptake rate, as is typical of fluid-phase uptake. Saturation of HRP adsorptive uptake occurs at about 25  $\mu\text{g}/\text{ml}$  (Fig. 3). This correlates well with a study of

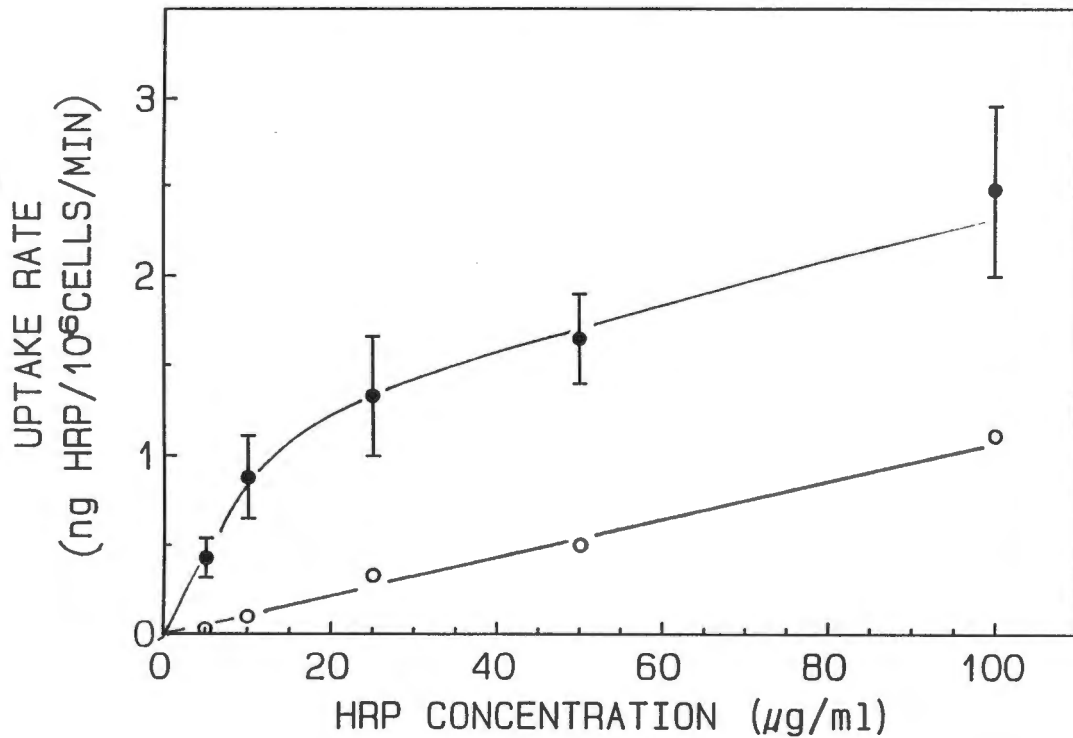


**FIG. 3. Concentration dependence of HRP pinocytosis**

Cells were pre-equilibrated at 37°C for 15 minutes, after which the indicated concentrations of HRP with (○) or without (●) yeast mannan (2 mg/ml) was added at time zero. Samples were taken at 20, 40 and 60 minutes to determine the rate at which HRP was taken up by the cells. Data obtained for cells incubated in the absence of mannan were the average of two experiments with error bars indicating systematic variation. Results for cells in the presence of mannan are from a single experiment, and the slope of the linear concentration dependence corresponds to a fluid uptake rate of 10  $\mu\text{m}^3/\text{cell}/\text{min}$  (cf. Fig. 2).

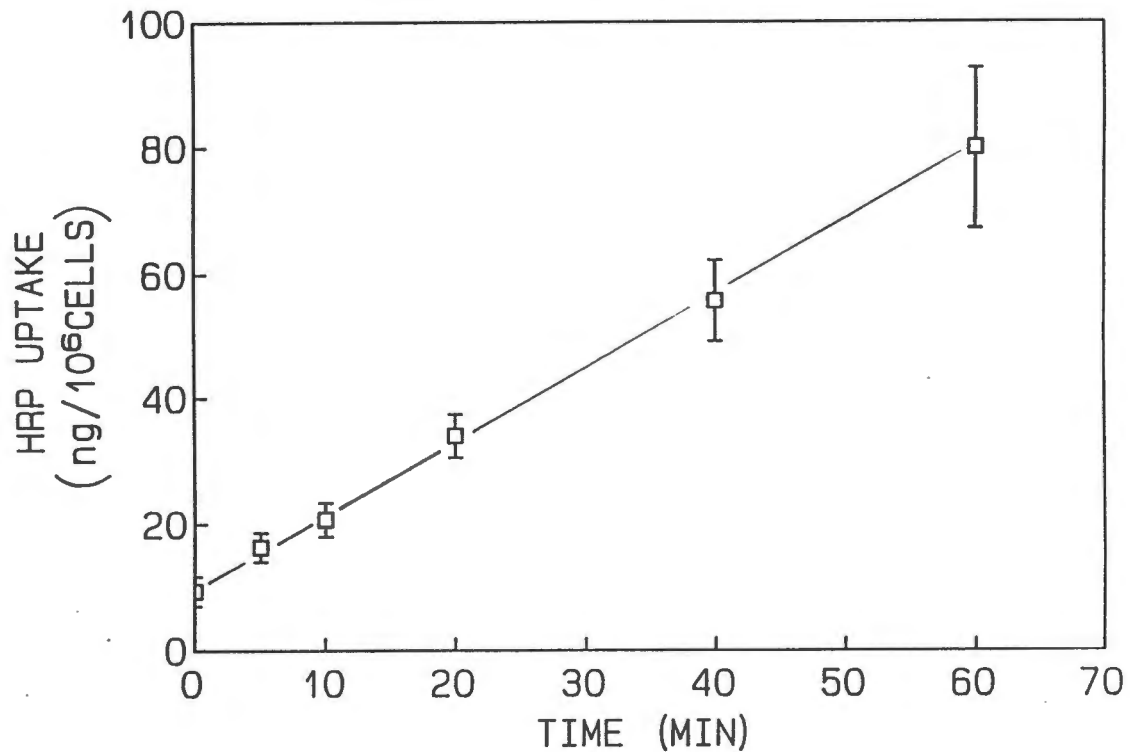


**FIG. 4. Adsorptive uptake of HRP**

Cells ( $5 \times 10^6/\text{ml}$ ) were equilibrated at  $37^\circ\text{C}$  for 15 min prior to their incubation at  $37^\circ\text{C}$  with HRP ( $25 \mu\text{g}/\text{ml}$ ). Samples of  $2.5 \times 10^6$  cells were taken at the indicated times, washed, and cell associated HRP measured. The data points are the average of seven independent experiments, error bars (formally S.E.M.) indicating systematic variation between individual experiments. The slope corresponds to an uptake rate of  $1.165 \text{ ng}/10^6 \text{ cells}/\text{min}$ .

mannose receptor-specific uptake of HRP in mouse bone-marrow-derived macrophages (47). These results suggest a mannose receptor-dependent uptake of HRP at concentrations below 25  $\mu\text{g/ml}$ .

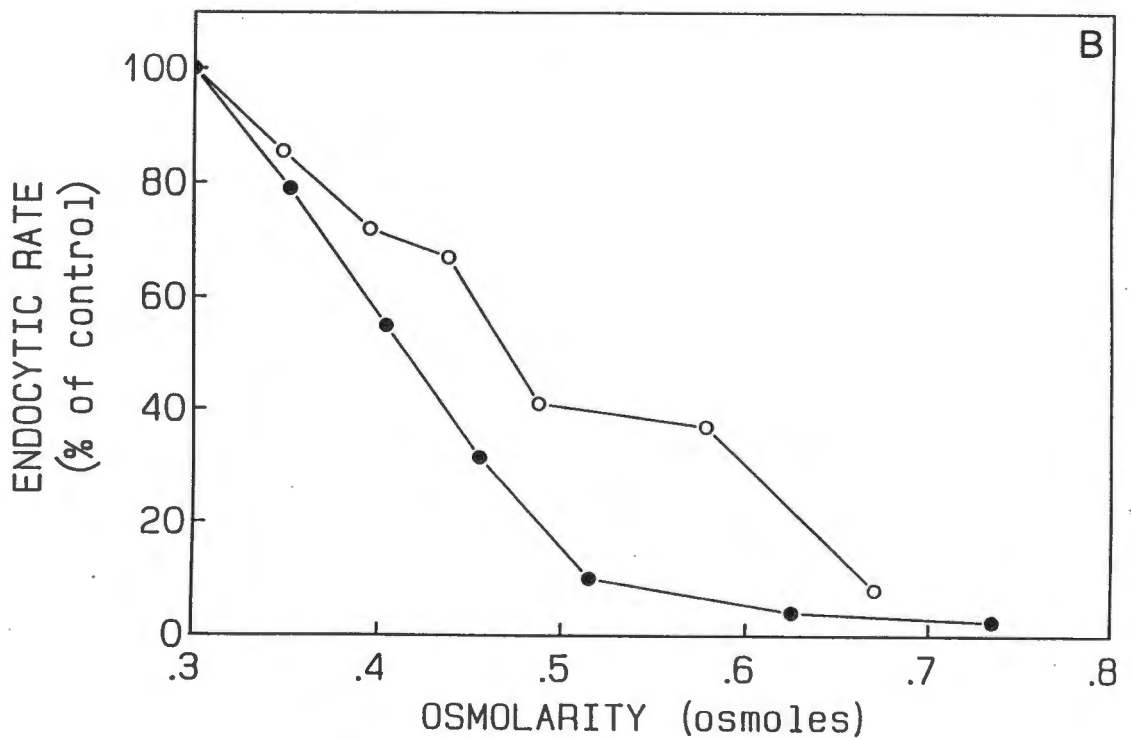
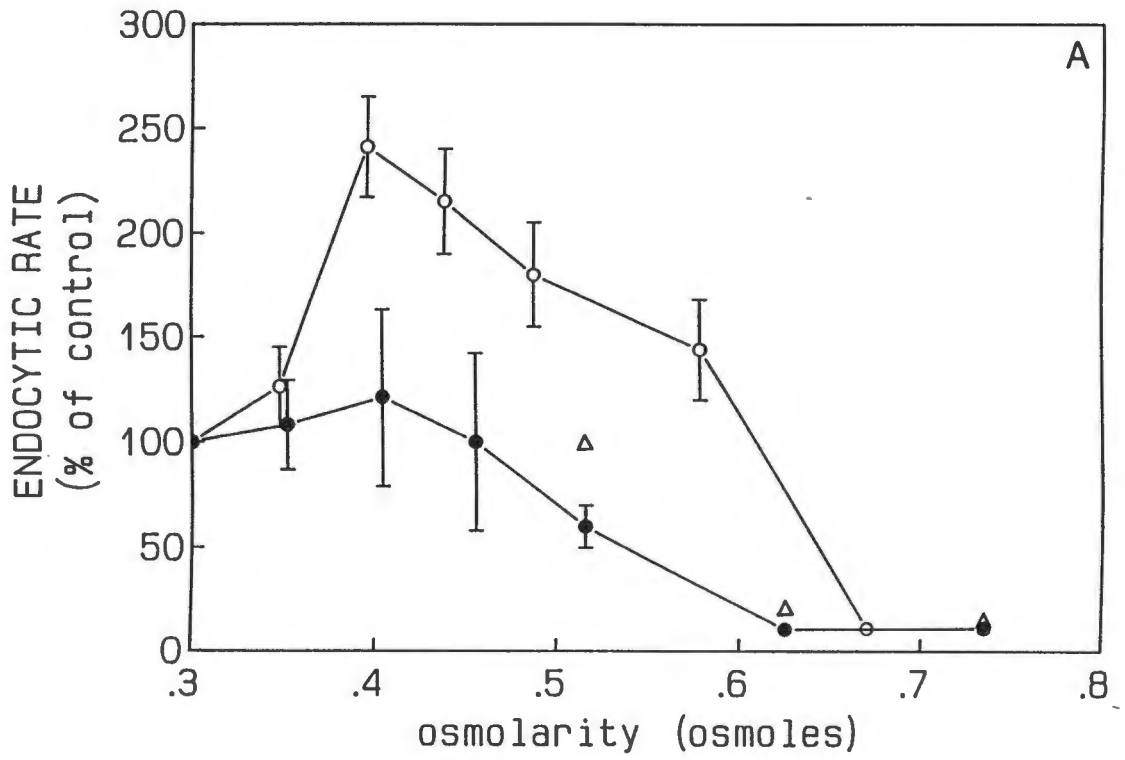
The merits of using HRP as a receptor-mediated endocytosis marker are apparent, as it is relatively cheap, safe (non-radioactive), sensitive and easily quantifiable. The kinetics of receptor-mediated uptake of HRP were determined using HRP at 25  $\mu\text{g/ml}$  (Fig. 4) (the contribution by fluid phase uptake at this concentration is negligible, see Fig. 3). The resultant uptake of  $1.165 \text{ ng}/10^6 \text{ cells/min}$  is linear over the sixty minutes measured, indicating that insignificant retroendocytosis occurred. The value at time zero is due to absorbance in the spectrophotometer because of a small amount of cell debris in the sample. A similar reading was obtained with the cells of a negative control.

#### The effect of hyperosmolarity on fluid-phase and HRP receptor-mediated endocytosis

In order to determine the effect of hypertonicity on receptor-mediated and fluid-phase uptake in P388D1 macrophages, cells were subjected to a range of increasing osmolarities, and the rate of HRP receptor-mediated, and FITC-dextran fluid-phase endocytosis, measured (Fig. 5A and 5B). Two well-known osmolites were used to effect the change in the osmolarity of the medium (i.e. NaCl and sucrose) (25,27). These were added to HerPMI to increase the osmolarity. The data in Fig. 5A show the effect of NaCl and sucrose-induced osmolarity increase on

net fluid-phase uptake as measured between 20 and 60 minutes. The effect on the initial fluid-uptake rate is shown for sucrose-induced hyperosmolarity. There was notably a significant difference in the effect of the two solutes on this process. In both cases, however, osmolarities above 0.634 osm inhibited fluid-phase endocytosis by 90%. The effect on the initial fluid-phase rate only becomes apparent above 0.52 osm. Sodium chloride is both an osmolite and an electrolyte, and thus its effects on the cell may be complex, whereas sucrose is more likely to act solely as an osmolite. This may explain the quantitative difference observed for the two solutes, with respect to the effect of their increasing osmolarities on fluid-phase uptake. The enhancement of fluid-phase uptake by the NaCl-induced osmolarity increase was noteworthy, reaching a maximum of 2.5 times the isotonic rate at 0.4 osm (Fig. 5A). This enhanced uptake was specific to NaCl, rather than a general osmotic effect, as sucrose failed to produce any significant increase in uptake rate over the same osmolarity range.

The effect on receptor-mediated uptake of HRP was markedly different from that on fluid-phase endocytosis. Data in figure 5B show a progressive inhibition of receptor-mediated uptake of HRP with increasing osmolarity. Sucrose-induced hypertonicity had a greater inhibitory effect than did NaCl, and reached 90% inhibition by 0.52 osm (i.e. HeRPMI + 200 mM sucrose). Thus by selecting the correct osmolarity, receptor-mediated endocytosis could be totally inhibited, without inhibition of the initial



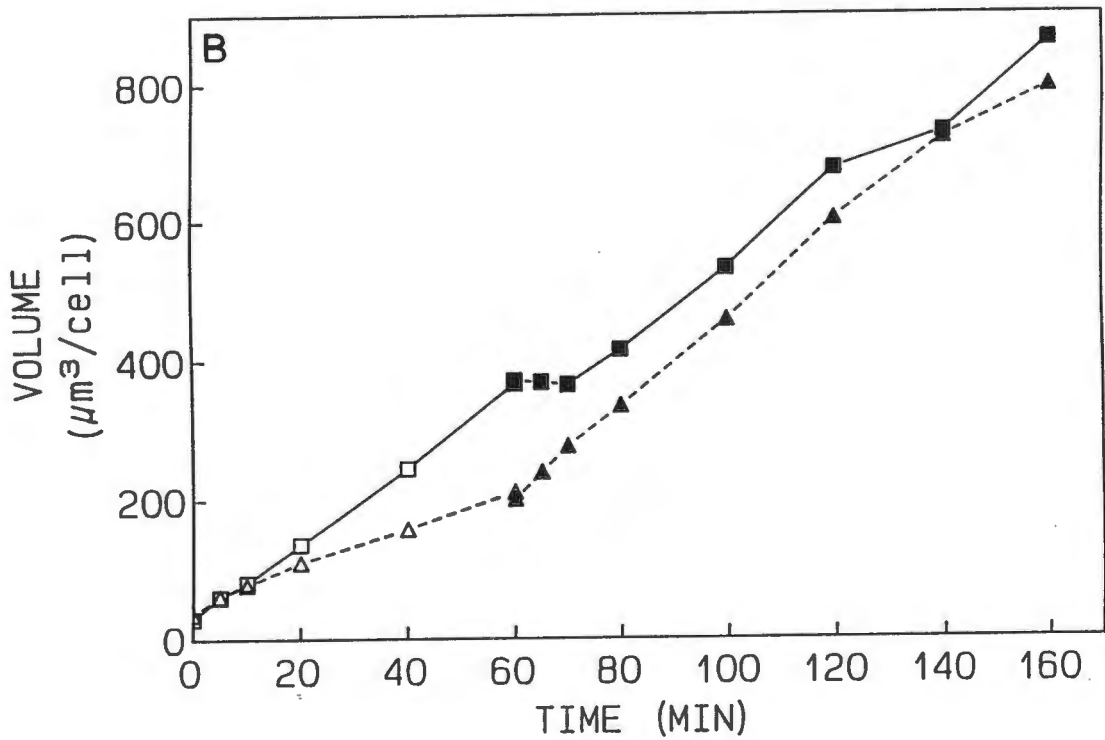
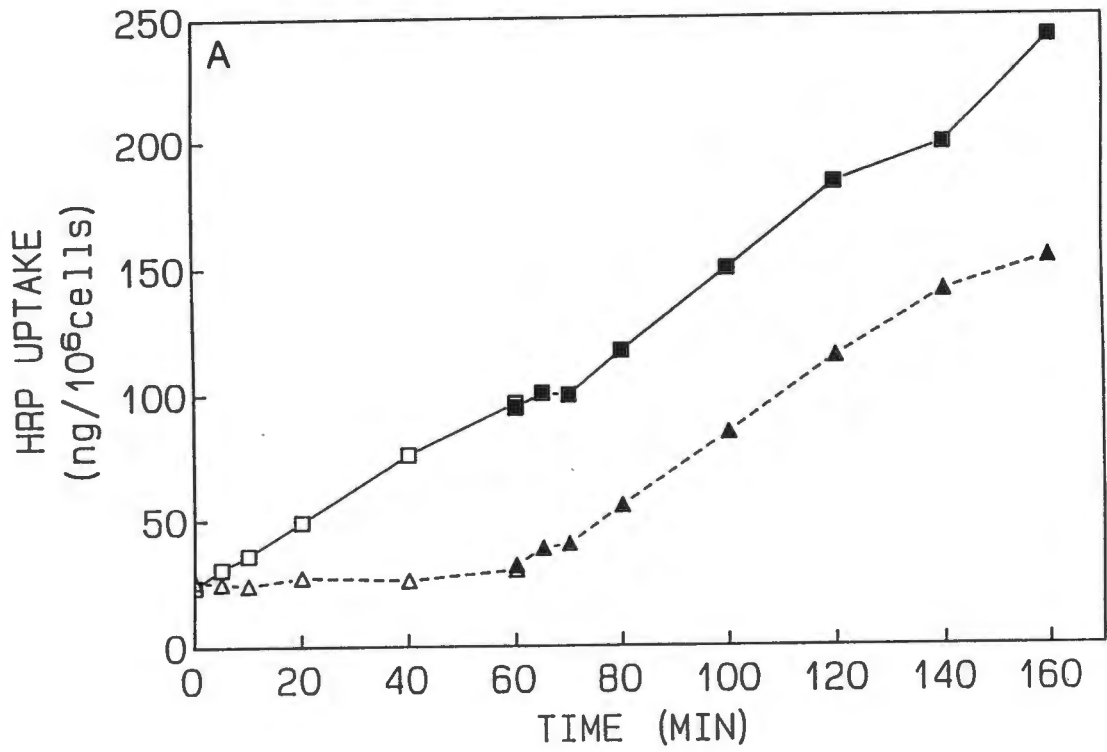
(LEGEND ON FOLLOWING PAGE)

FIG. 5. Effect of osmolarity on endocytic uptake

A: Fluid-phase uptake: Cells ( $5 \times 10^6$ /ml) were incubated at  $37^\circ\text{C}$  with FITC-dextran (3 mg/ml) in HeRPMI, made hypertonic to varying degrees by the addition of either NaCl (o) or sucrose (●). They had previously been pre-equilibrated at  $37^\circ\text{C}$  for 15 min in the same medium before the addition of FITC-dextran. Samples of  $2.5 \times 10^6$  cells were removed at 20, 40 and 60 minutes to determine the rate of uptake over this period. The rate was expressed as a percentage of the rate under isotonic conditions. Data are the average of two experiments, showing systematic variation between experiments. Cells remained  $> 85\%$  viable, as determined by the exclusion of trypan blue, even after 60 minutes at the high osmolarities. Cell viability was about 5% greater in sucrose than in NaCl. ( $\Delta$ ) indicates the initial rate of endocytosis as measured between 0 and 10 mins of uptake.\* Sucrose was chosen as the osmolite for this measurement.

B: HRP adsorptive endocytosis: An experiment was done as for Fig. 5A, but FITC-dextran was replaced with HRP (25  $\mu\text{g}/\text{ml}$ ). All data points are from a single experiment.

(\* Single experiment - For initial rate vs net rate cf. Fig. 6B )



(LEGEND ON FOLLOWING PAGE)

FIG. 6. Reversibility of the hypertonic effect

Cells ( $5 \times 10^6$ /ml) were pre-equilibrated in either isotonic (0.3 osm) HeRPMI ( $\square$ ) or hypertonic (0.52 osm) HeRPMI ( $\Delta$ ) for 15 min at 37°C. HRP (25  $\mu$ g/ml) in A and FITC-dextran (3 mg/ml) in B was then added to cells at 37°C at time zero. 0.5 ml samples were removed at the indicated time points to determine cell associated marker. After 60 minutes the cultures were rapidly cooled to 4°C by diluting into 5 volumes of ice-cold HeS, and immediately pelleted at 150 x g for 5 min and resuspended in isotonic medium containing the same concentration of marker as before at 4°C. After rapidly warming to 37°C, samples were again removed at the indicated times and cell associated marker was measured (filled symbols).\*

(\* Single experiment)

fluid-phase uptake rate, and only a partial (48%) inhibition of net fluid uptake.

Cell viability as determined by trypan blue exclusion, was greater than 90% throughout the experiment when using sucrose as the osmolite, and greater than 85% if NaCl was used. Sucrose-induced hypertonicity was more gentle on the cells and was less likely to have complicated electrolytic effects, following which it was decided to use sucrose-HeRPMI at 0.52 osmoles for all further hypertonicity studies. Under these conditions fluid-phase and receptor-mediated endocytosis were routinely inhibited by 0% and 90% respectively.

The inhibitory effect of hypertonicity at 0.52 osm could be reversed by resuspending the cells in isotonic medium, after 5 minutes at 4°C to effect a change in the medium (Fig. 6A and 6B). The rates of uptake returned to normal immediately, for both fluid-phase and receptor-mediated endocytosis. Cooling of the cells to 0°C to facilitate changing of the medium after 60 minutes, seemed to induce a lag in uptake following warming to 37°C. This lag effect was seen for both modes of uptake, but was absent in the cells previously incubated in hypertonic medium.

HRP was shown to be unsuitable for fluid-phase uptake studies when used on its own. The addition of yeast mannan however, prevented binding to the mannose receptor, allowing HRP to be taken up in a true fluid-phase fashion. In the absence of

mannan, HRP was taken up by receptor-mediated endocytosis with a rate of  $1.165 \text{ ng}/10^6 \text{ cells}/\text{min}$  at  $25 \text{ } \mu\text{g}/\text{ml}$ .

This rate was equivalent to the internalization of 17500 HRP molecules/cell/min, which corresponds to a cell surface population of about 50 000 mannose receptors, assuming an average surface residence time of a receptor to be approximately 3 minutes (20). Such a population is compatible with results obtained for rat alveolar macrophages indicating  $10^5$  surface receptors/cell (50).

Endocytosis of HRP at  $25 \text{ } \mu\text{g}/\text{ml}$  included a fluid-phase contribution of 20% (Fig. 3). Inhibition of receptor-mediated uptake of HRP would thus reach a maximum of 80% at  $25 \text{ } \mu\text{g}/\text{ml}$  if fluid-phase uptake had been unaffected. In view of a 40% inhibition of net fluid uptake, an 88% maximum inhibition of HRP uptake at  $25 \text{ } \mu\text{g}/\text{ml}$  could be expected. The data in Figs. 3 and 5 suggest that sucrose-induced hypertonicity at 0.52 osm fully inhibited receptor-mediated uptake of HRP.

The above results confirmed that hypertonicity selectively and reversibly inhibited receptor-mediated uptake at osmolarities around 0.52 osm, as previously reported for hepatocytes (51,52). Further increase in osmolarity inhibited fluid-phase uptake as well, confirming the finding in fibroblasts (36,53), but contrary to results obtained for polymorphonuclear leucocytes (34). Such selectivity of inhibition suggested that fluid-phase and receptor-mediated uptake occurred via independent mechanisms.

The effect of sucrose-induced hyperosmolarity on HRP binding at the cell surface

An obvious explanation for the inhibitory effect of hypertonicity on receptor-mediated HRP uptake was that elevated concentrations of sucrose or NaCl inhibited binding of HRP to the mannose-fucose receptor. In the case of hepatocytes, hypertonicity inhibited uptake of asialoglycoproteins (ASGP) via the ASGP receptor, without any effect on binding of this ligand to its receptor (25). In the present study, binding of HRP to its receptor on the surface of P388D1 macrophages was investigated.

A number of techniques were used to measure surface binding of HRP at 4°C. All involved the use of either  $^{125}\text{I}$ -HRP, or unlabelled HRP as assayed enzymatically. Ligand was incubated with the cells for up to 3 hours at 4°C, followed by washing to remove unbound ligand. It was this washing step that was altered in each case, in order to detect specific binding. Although these techniques turned out to be totally unsuccessful, they are briefly listed below.

1) Incubation of HRP at 4°C with suspended cells followed by washing three times by pelleting the cells at 150 x g for 5 min and resuspending in fresh HeS.

Result: No specific binding of  $^{125}\text{I}$ -HRP as determined by using competitive concentrations of mannan. Non-specific binding varied greatly and unlabelled HRP was barely detectable by enzymatic assay. Washing of suspended cells took approximately

45 minutes, and thus bound HRP might already have dissociated from the receptor during washing. A faster washing technique was thus required.

2) Incubation at 4°C with attached cells which could be washed very rapidly (four washes within 15 minutes). Specific binding of both  $^{125}\text{I}$ -HRP and unlabelled HRP failed to be detectable, in view of high non-specific binding to the dish, even in the presence of 1% BSA.

3) (Silicon oil wash) Suspended cells could be washed by passage through a layer of silicon oil (21). This technique required cells to be layered on top of a silicon oil cushion in a 0.5 ml Eppendorf tube, followed by rapid (< 30 sec) centrifugation through the oil to form a pellet at the bottom of the tube with the extracellular fluid remaining above the oil. Clumping of the cells appeared to trap excess ligand when the cells were spun through the oil, and thus there was an extremely high background. Attempts to prevent this by using lower cell concentrations and BSA were unsuccessful.

Since specific binding of HRP to the cell surface at 4°C could not be measured (possibly for technical reasons), cell surface binding at 37°C was measured. Cells were incubated with HRP at 37°C for 5 minutes. They were then washed at 4°C to remove unbound ligand, and subjected to a low pH wash at 4°C to release surface-bound HRP which could be measured (43).  $^{125}\text{I}$ -HRP failed to produce any specific binding, as for the previous three techniques, and there was a high degree of non-specific

binding. This could be due to damage to the HRP by the iodination procedure, which might have exposed hydrophobic sites which bind avidly to the cell surface. Unlabelled HRP on the other hand did produce significant specific binding. Non-specific binding amounted to only 10-20% of specific binding. HRP binding, as determined by its concentration dependence (Fig. 7A), showed low affinity, mannan inhibitable binding of HRP ( $K_d$   $10^{-6}M$ ) to 20000 sites per cell surface.

This binding could be inhibited by 65% under hypertonic (0.52 osm) conditions (Fig. 7B). Although only one experiment was performed for sucrose-induced hypertonic conditions (Fig. 7B) and only at one concentration of HRP (25  $\mu g/ml$ ), the result strongly suggested that inhibition of HRP binding, rather than coated-pit formation, was the cause of reduced HRP uptake under hypertonic conditions.

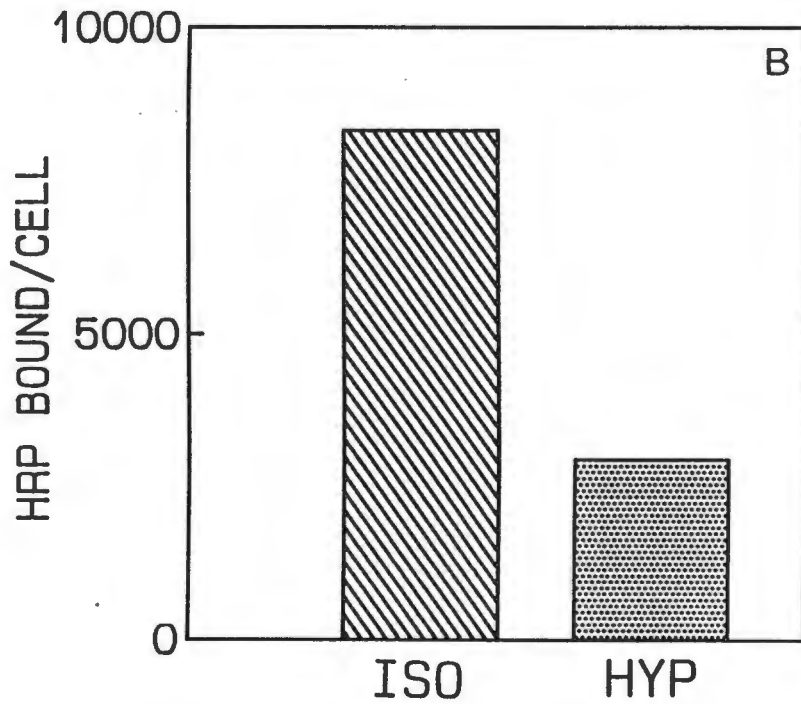
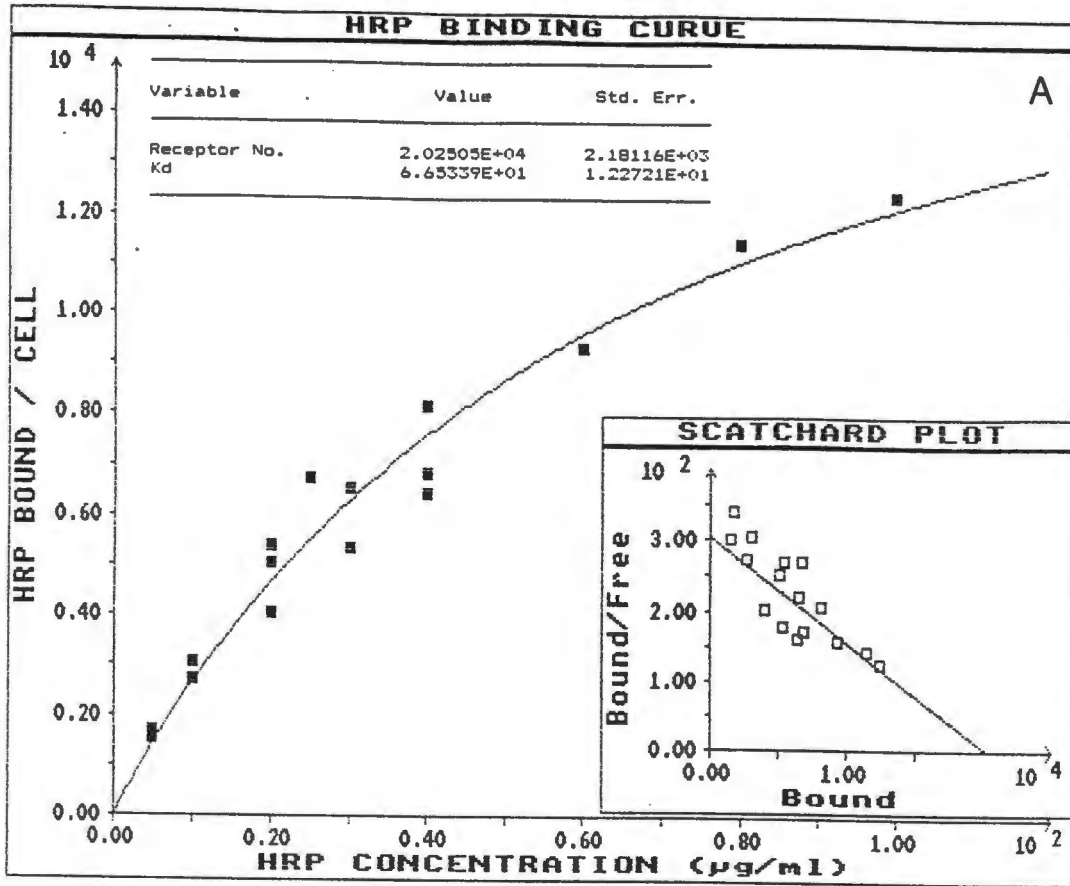
Even though it was reported that cell-line macrophages P388D1 and J774, had no or few mannose receptors (64), the result in Fig. 3 clearly showed an enhanced uptake of HRP at low concentrations, which was inhibitable by excess yeast mannan. These results were compatible with those obtained for mannose receptor-mediated uptake in mouse bone marrow-derived macrophages (47). The cell surface-receptor number of  $20-50 \times 10^3$  and the binding affinity ( $K_d$   $10^{-6} - 10^{-7} M$ ), obtained via binding at  $37^\circ C$  or endocytic uptake rates, were both slightly lower than the values of  $10^5$  and ( $10^{-9} M$ ) as reported for differentiated macrophages (50).

The present results on receptor number would have to be checked by a specific antibody to the putative mannose receptor. The fact that HRP binding was mannan inhibitable suggested that it occurred via mannose or saccharide specific sites. This could explain why sucrose-induced hypertonicity inhibited uptake to a greater extent than sodium chloride.

#### The effect of hypertonicity on transferrin receptor-mediated endocytosis

To determine the effect of hyperosmolarity on receptor-mediated endocytosis, it was necessary to measure the effect in more than one receptor uptake system. Transferrin endocytosis is a well documented coated-pit-mediated uptake system, and is almost universal amongst higher order animals. It therefore would make a good candidate as an alternative to HRP to measure receptor-mediated uptake.

Cells were incubated at 37°C with  $^{125}\text{I}$ -transferrin ( $^{125}\text{I}$ -Tf), at a concentration of 33 nM, to measure receptor-mediated uptake of this ligand. Non-specific uptake was determined by measuring uptake of  $^{125}\text{I}$ -Tf in the presence of 1  $\mu\text{M}$  unlabelled transferrin (i.e. 30 fold excess). The effect of osmolarity on uptake was then determined for 0.52, 0.63 and 0.74 osm, by adding 200, 300



(LEGEND ON FOLLOWING PAGE)

**FIG. 7. HRP binding**

**A:** Cells were incubated with HRP at the various concentrations indicated for 5 min at 37°C. The amount of HRP associated with the cell surface was then determined via release by an acid wash. The indicated values (■) represent individual results minus non-specific binding, as determined by the addition of excess mannan. A binding curve was obtained by non-linear regression. Scatchard analysis (insert) indicated that binding occurred with an affinity of  $K_d \sim 10^{-6}$  M, to about 20000 sites per cell surface.

**B:** Effect of hypertonicity on HRP binding: Cells were incubated with HRP at 25 µg/ml in either HeRPMI or HeRPMI + 200 mM sucrose (0.52 osm) for 5 min at 37°C, and surface binding was determined as in A:. The result of a single experiment is shown.

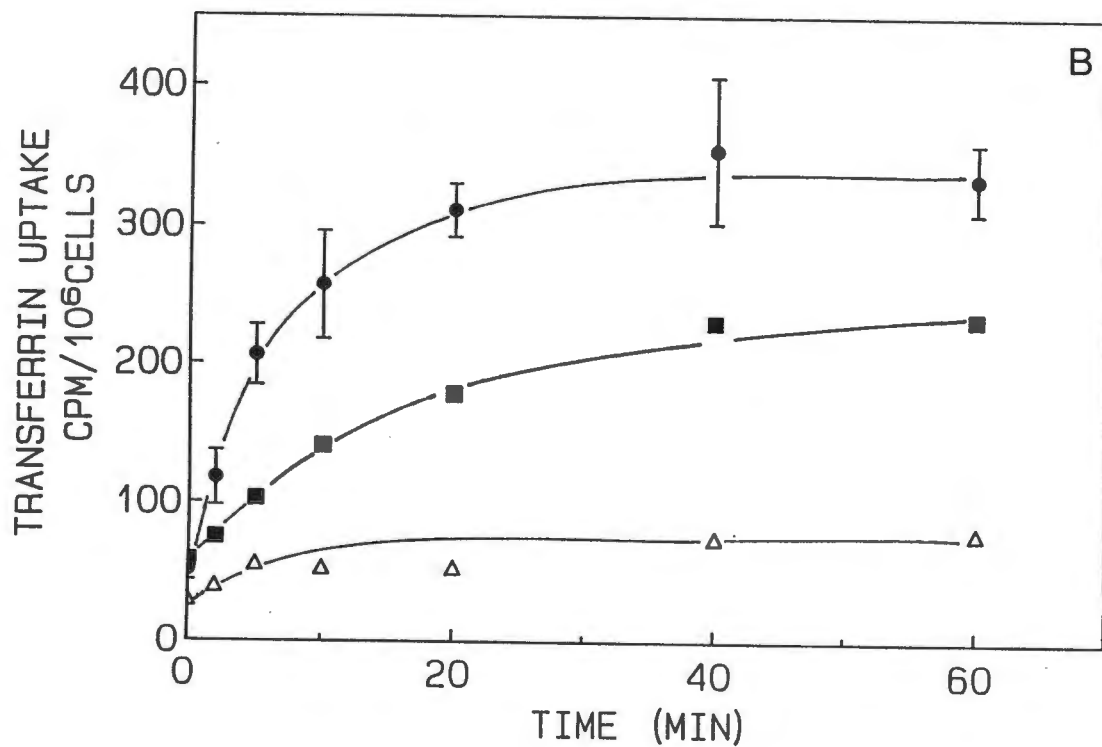
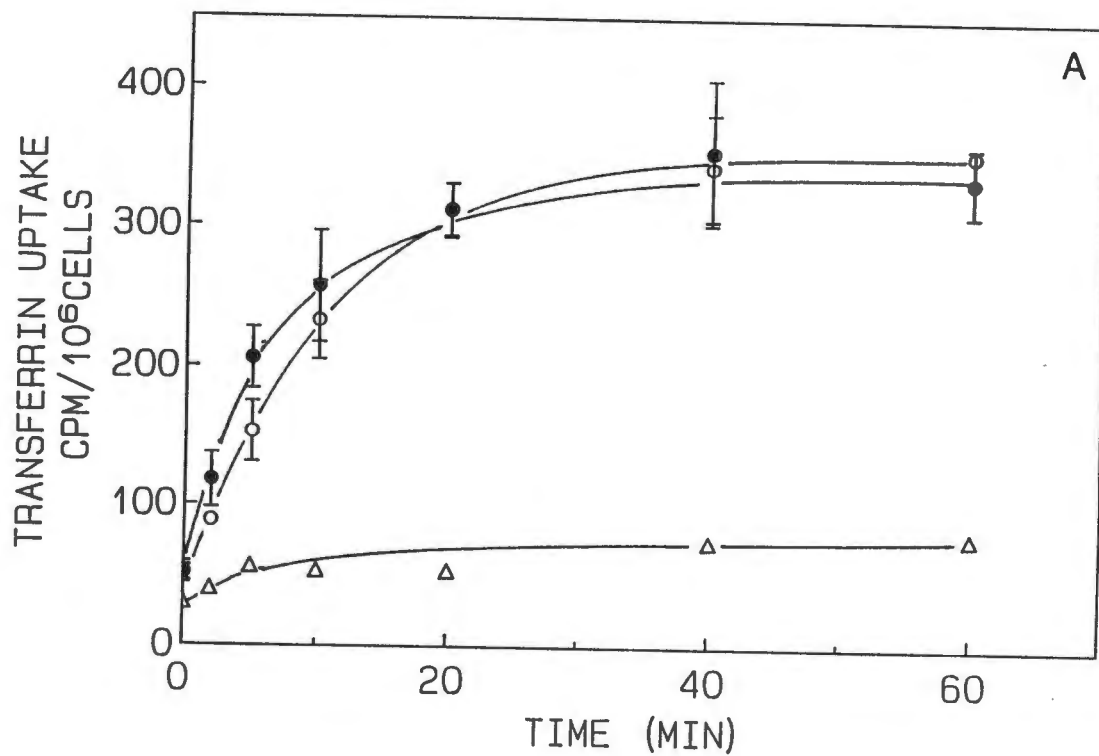
and 400 mM sucrose to HeRPMI respectively (Fig. 8A,B,C). Fluid-phase uptake was measured simultaneously with FITC-dextran (Fig. 8D).

Sucrose-induced hyperosmolarity at 0.52 osm affected transferrin uptake only slightly (Fig. 8A), unlike its inhibiting effect on receptor-mediated uptake of HRP (Fig. 5B). The initial rate of transferrin uptake was slowed to 56% of the isotonic rate (1600 vs 2800 transferrin molecules/cell/min) under 0.52 osmolar conditions. However, a steady state was reached at the same level (330 cpm/10<sup>6</sup> cells) as that of isotonic uptake. Non-specific uptake was about 20% of that of specific uptake (Fig. 8A). Increasing the osmolarity to 0.63 osm (HeRPMI + 300 mM sucrose) had a notable effect on <sup>125</sup>I-Tf uptake, both in extent and rate of uptake (26% of Control). The time course of this experiment was only 60 minutes and thus it was not determined if the internal pool reached the same capacity as isotonic uptake, or whether it was reduced by the osmolarity shift. A greater degree of inhibition was achieved by increasing the osmolarity to 0.74 osm (HeRPMI + 400 mM sucrose) (Fig. 8C). Again both the rate (22% of control) and extent of uptake was reduced relative to values at the lower osmolarities. It appeared that the size (i.e. steady state level) of the internal pool of transferrin was reduced by the increase in osmolarity. The saturation level of 330 cpm/10<sup>6</sup> cells amounted to  $24.5 \times 10^3$  transferrin molecules/cell. This was similar to values reported for another mouse cell type, teratocarcinoma stem cells (45), which

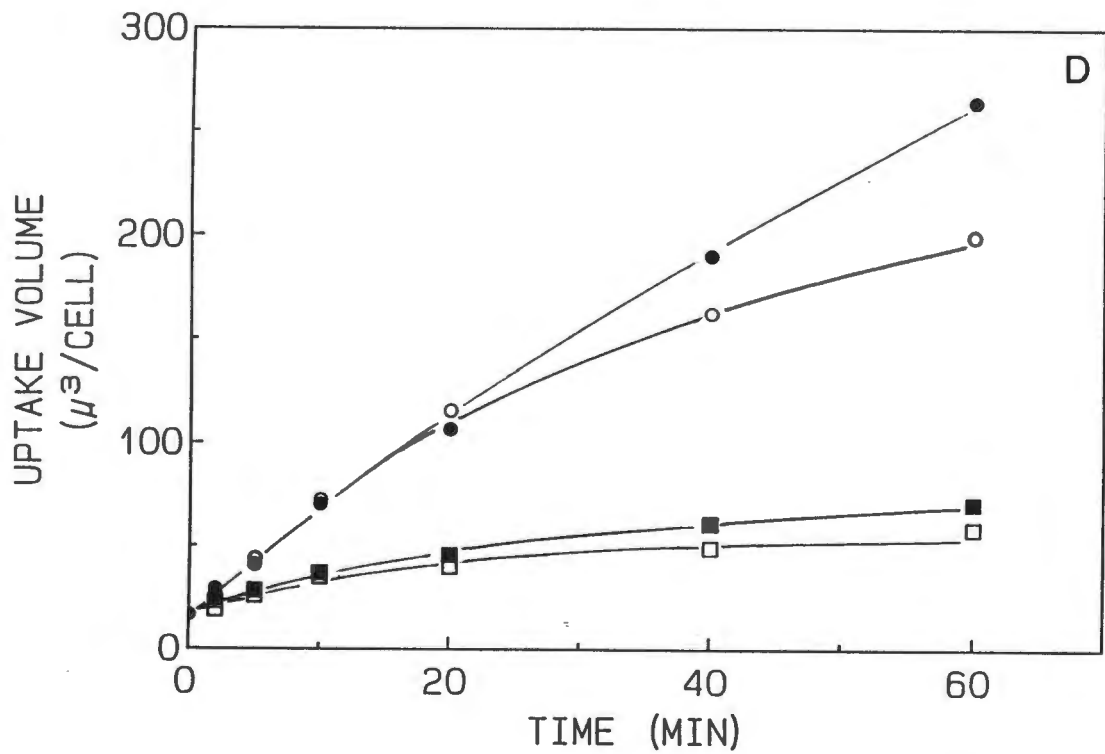
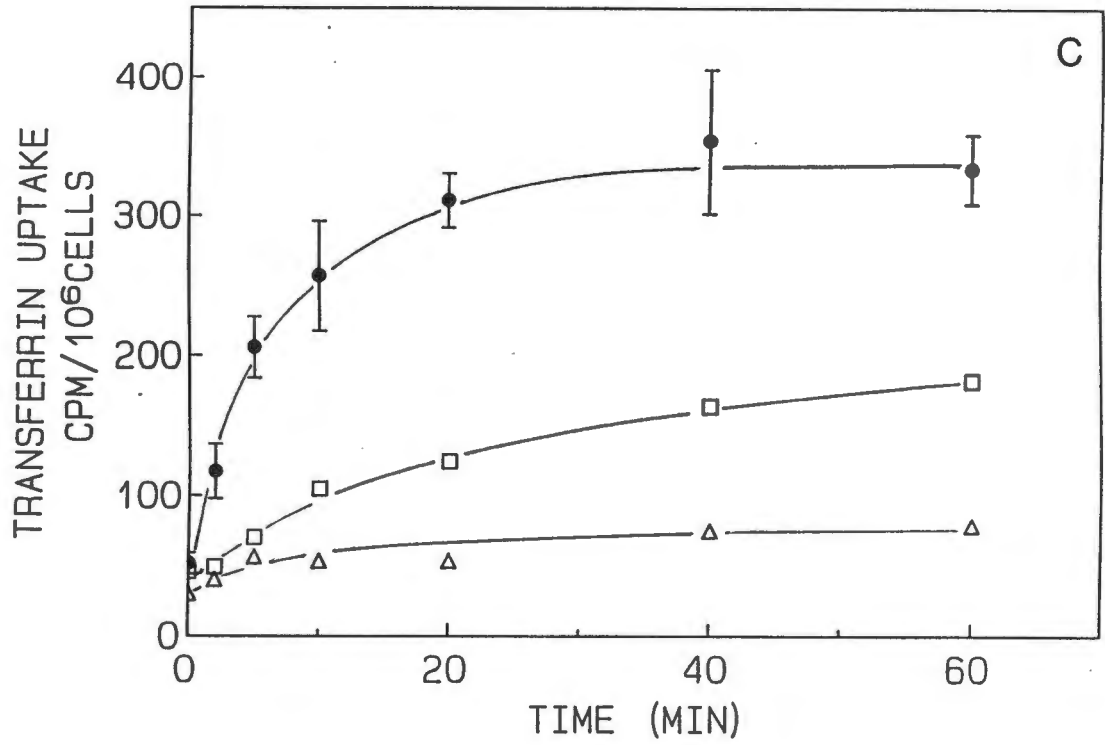
showed a surface receptor number of  $5.7 \times 10^3$  and an internal to external ratio of 3:1.

The concomitant uptake of fluid-phase marker (Fig. 8D) was also inhibited by the increasing osmolarity (as in Fig. 5), in a very similar manner to transferrin uptake. Increasing osmolarity appeared to induce biphasic kinetics to fluid-phase uptake. The fluid uptake rate at 0.52 osm was the same as the isotonic rate for the first 20 minutes, after which there was a notable drop in the net rate to about 52% of the rate at isotonicity. This could be due to retroendocytosis of fluid. The effects of increasing osmolarity above 0.52 osm on the initial rate of fluid and transferrin uptake were very similar with the greatest shift in inhibition occurring between 0.52 and 0.63 osm in both cases. This suggested a common mode of inhibition, viz. inhibition of endocytosis in general.

Hypertonicity could have affected binding to the receptor, however any significant inhibitory effect was seen only at osmolarities above 0,52 osm. Binding studies will still have to be performed to confirm this.



(LEGEND ON PAGE 49)



(LEGEND ON FOLLOWING PAGE)

Fig. 8. Effect of osmolarity on transferrin uptake vs fluid-phase uptake

Cells ( $10 \times 10^6$ /ml) were pre-incubated at  $37^\circ\text{C}$  in HeRPMI made hypertonic to varying degrees by the addition of sucrose, for 15 minutes.  $^{125}\text{I}$ -Transferrin ( $^{125}\text{I}$ -Tf) (33 nM) and FITC-dextran (3 mg/ml) were added to the cells at  $37^\circ\text{C}$  and samples of  $2.5 \times 10^6$  cells removed at the indicated times. These were cooled rapidly by diluting into 10 volumes of ice-cold HeS. The cells were washed and measured for FITC-dextran and  $^{125}\text{I}$ -Tf.

A:  $^{125}\text{I}$ -Tf uptake in HeRPMI ( $\bullet$ ), HeRPMI + 200 mM sucrose ( $\circ$ ) or in HeRPMI + 1  $\mu\text{M}$  unlabelled Tf ( $\Delta$ ). Average of two experiments  $\pm$  S.E.M..

B:  $^{125}\text{I}$ -Tf uptake in HeRPMI + 300 mM sucrose ( $\blacksquare$ ). Result of a single experiment. ( $\bullet$  and  $\Delta$ ) data as in A).

C:  $^{125}\text{I}$ -Tf uptake in HeRPMI + 400 mM sucrose ( $\square$ ). Single experiment ( $\bullet$  and  $\Delta$ ) data as in A).

D: Fluid-phase uptake of FITC-dextran in HeRPMI ( $\bullet$ ), HeRPMI + 200 mM sucrose ( $\circ$ ), in HeRPMI + 300 mM sucrose ( $\blacksquare$ ) or in HeRPMI + 400 mM sucrose ( $\square$ ). Data were from a single experiment (cf. Fig. 2).

Note: "uptake" refers to intracellular and surface-bound label.

CHAPTER 4INTERNALIZATION OF <sup>3</sup>H-GALACTOSE LABELLED PLASMA-MEMBRANE GLYCOCONJUGATESRESULTS AND DISCUSSION

The aim of this project was to determine whether fluid-phase and receptor-mediated endocytosis involved different sized primary pinosomes as measured by relating the rates of volume uptake and membrane internalization.

The approach was to measure both the rate of membrane internalization and concomitant fluid uptake, under isotonic conditions and under hypertonic conditions where coated vesicle formation could be selectively inhibited (0.52 osm). Such inhibition, although not complete, was totally selective for receptor-mediated endocytosis. This result would indicate the contribution of the coated-pit-mediated pathway to general plasma-membrane internalization as well as the volume-weighted average diameter of pinosomes not involved in this form of uptake.

The rate of membrane internalization can be measured via the kinetics of redistribution of a plasma-membrane marker to the intracellular membranes. The kinetics of membrane internalization have been previously reported for P388D1 macrophages by using radioactive galactose, covalently attached to cell-surface glycoconjugates as a membrane marker (32) (cf. Chapter 1). The membrane is internalized into two consecutive

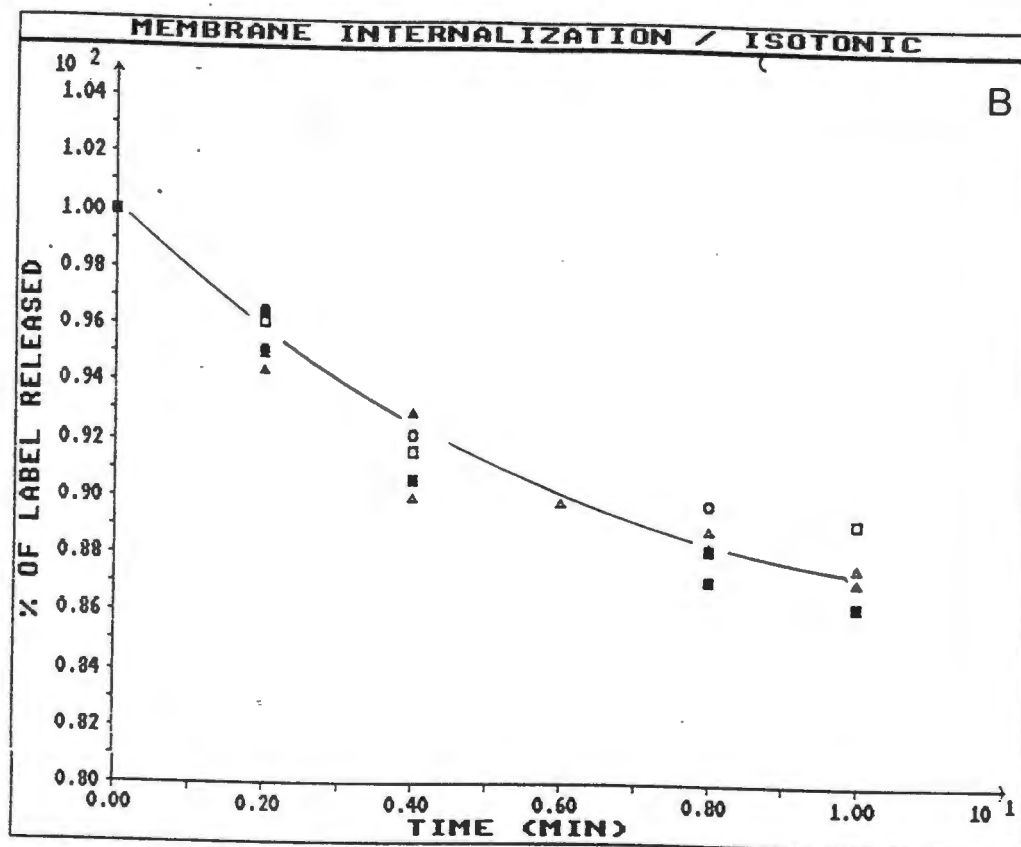
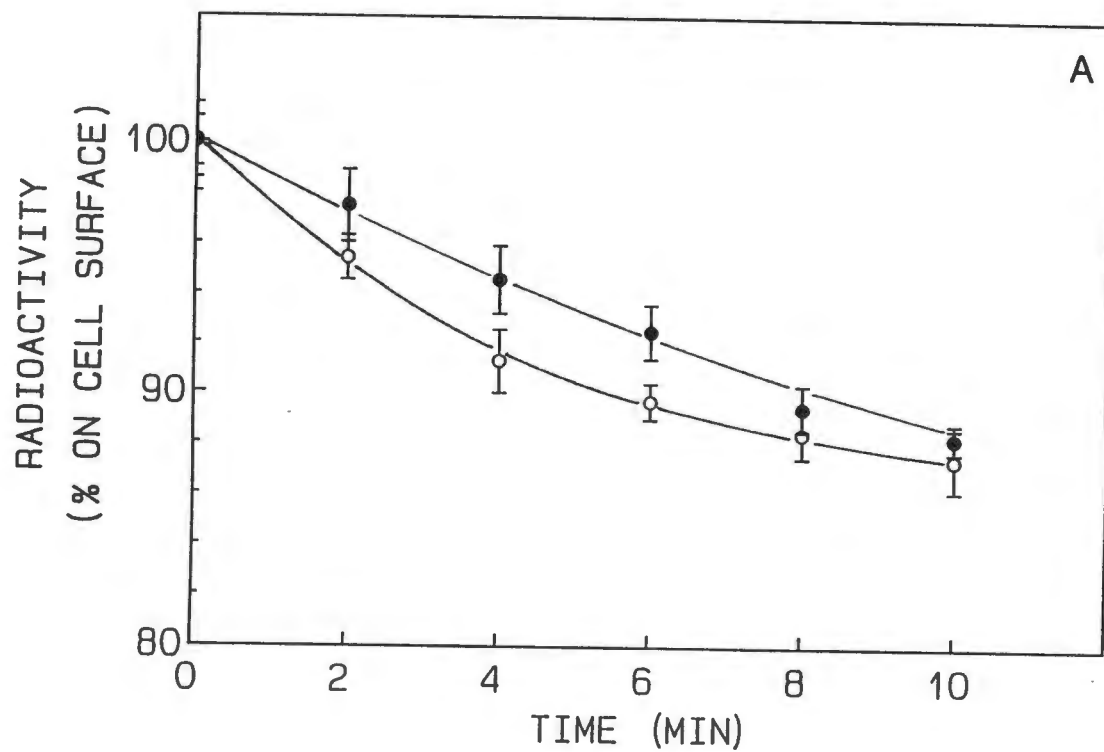
internal compartments, viz. the endosomal and lysosomal compartments. The same plasma-membrane labelling technique was adopted for this study.

#### Membrane internalization under hypertonic conditions

The main interest was to study membrane-flow kinetics from the plasma membrane into the endosomal compartment. The redistribution of label was thus only measured over the first 10 minutes at 37°C, after cell surface labelling at 4°C. The time-dependent decrease of the fraction of label on the cell surface is shown in Fig. 9A, as observed for isotonic and hypertonic conditions respectively. The data could be analysed in terms of pseudo-first-order kinetics (Fig. 9B and C), to give the actual rate of membrane internalization at the cell surface (cf. Appendix).

The rate of internalization of plasma-membrane under isotonic conditions was 2.6%/min whereas the rate under hypertonic conditions (0.52 osm) was 1.5%/min, which was notably slower than the isotonic rate. The variation between individual experiments was not more than 3% as shown in Figures 9B and C.

The volume-weighted average diameter of pinocytotic vesicles formed under the two conditions was calculated using the rate of initial fluid uptake ( $3.75 \mu\text{m}^3/\text{cell}/\text{min}$ ) (Fig. 2) for both isotonic and hypertonic conditions, as the initial rate of fluid uptake under hypertonic conditions (0.52 osm) is the same as



(LEGEND ON FOLLOWING PAGE)

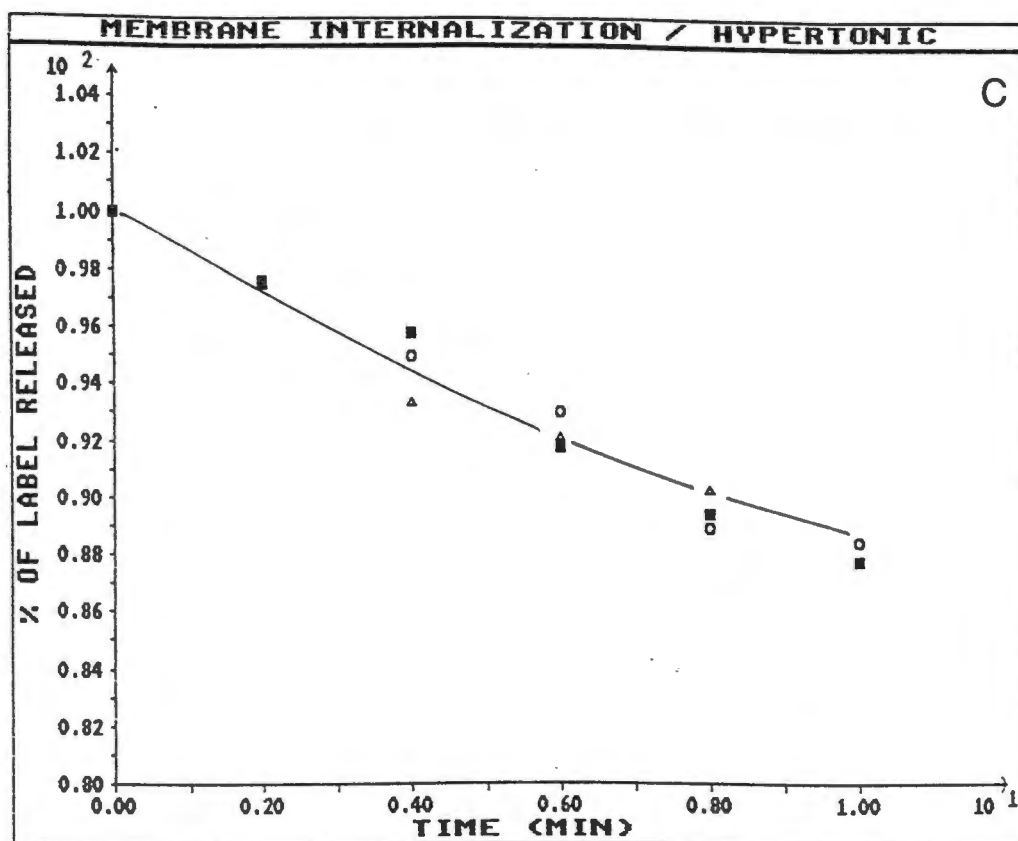


**FIG. 9. Effect of hypertonicity on membrane internalization**

Cells were labelled with UDP [6-<sup>3</sup>H]-galactose (Methods), and resuspended at  $5 \times 10^6$  cells/ml in HeRPMI (○) or in HeRPMI + 200 mM sucrose (●), at 0°C. Triplicate zero time samples (0.5 ml) were then removed and fixed in 2% glutaraldehyde before warming. The remaining cells were then warmed rapidly to 37°C and duplicate samples removed at the indicated times, and fixed as above. After washing in HeRPMI, the fixed cells were incubated with  $\beta$ -galactosidase (0.2 units/ml) overnight at room temperature, and samples removed and the radioactivity measured (Methods).

(A) Average of 5 experiments  $\pm$  S.E.M. and normalized to 100% on the cell surface at time zero. To show the inter-experimental variation, the results for individual experiments are plotted as separate symbols for isotonic (B) and hypertonic (C) conditions respectively.

that at isotonicity (Fig. 5A). An internalization rate of 2.6% of the plasma-membrane/min, is equivalent to the total plasma-membrane area being internalized every 38.5 minutes. In this time the cell takes up  $144.2 \mu\text{m}^3$  by fluid-phase pinocytosis, at a rate of  $3.75 \mu\text{m}^3/\text{cell}/\text{min}$ . The cell surface area of a P388D1 macrophage has been estimated to be  $1300 \mu\text{m}^2$  (32). Thus  $144.2 \mu\text{m}^3$  is enclosed in  $1300 \mu\text{m}^2$  of membrane, giving a surface to volume ratio of  $1300/144.2$ . Vesicle size can then be calculated as  $0.665 \mu\text{m}$  ( $6 \times \text{Volume}/\text{Surface area}$ ). In the same way, vesicle size under hypertonic conditions was calculated as  $1.15 \mu\text{m}$ , which was significantly larger than the average size at isotonicity.

The inferred pinosome diameter of  $0.66 \mu\text{m}$  was much larger than reported previously, viz.  $0.24 \mu\text{m}$ . However, the present data for both the internalization rate and the uptake rates were very similar to those in the previous reports, viz. 4.7% of the plasma/membrane/min and  $2.5 \mu\text{m}^3/\text{cell}/\text{min}$ , respectively (32). This would leave the cell surface area as the only parameter leading to a larger value for the average vesicle size. The cell surface area, previously estimated as  $1300 \mu\text{m}^2$  for P388D1 macrophages (32), was not assessed in the present investigation. Substituting a value of  $3600 \mu\text{m}^2$  would result in a vesicle size of  $0.24 \mu\text{m}$  as previously reported (32). In comparison, the surface area of another macrophage cell-line, J774, has been reported to be about  $3900 \mu\text{m}^2$  (cf. 20).

The calculation of membrane internalization rates, from the redistribution kinetics of membrane marker (Fig. 9), was based

on the assumption that all labelled plasma-membrane constituents were internalized to the same relative extent. This assumption seemed to be justified for endocytosis under isotonic conditions, as observed previously for the present labelling system, as well as for iodinated plasma/membrane proteins in J774 macrophages (60). The above assumption had to be tested for hypertonic conditions, as inhibition of coated-pit formation might prevent the internalization of certain cell-surface molecules.

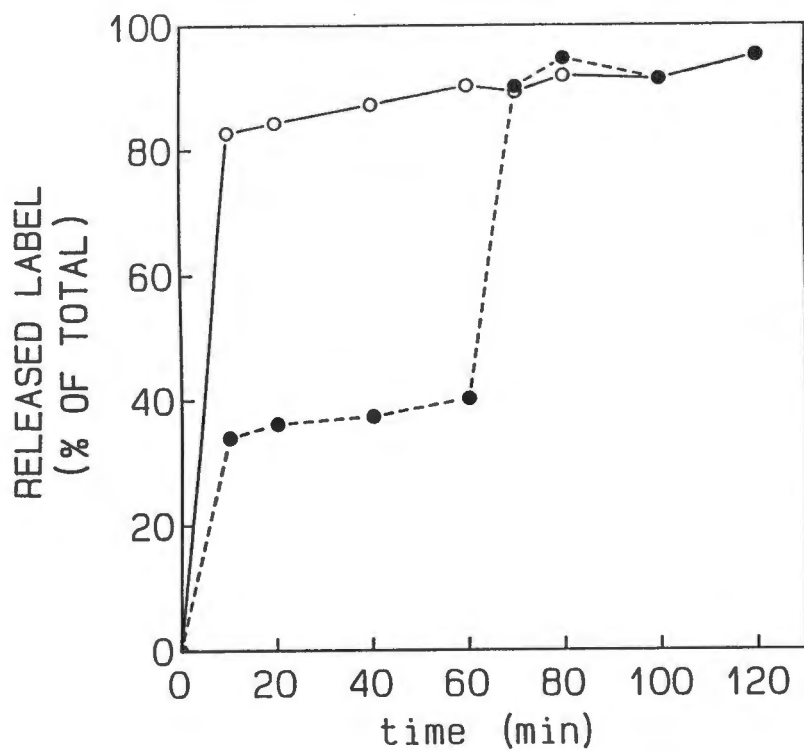
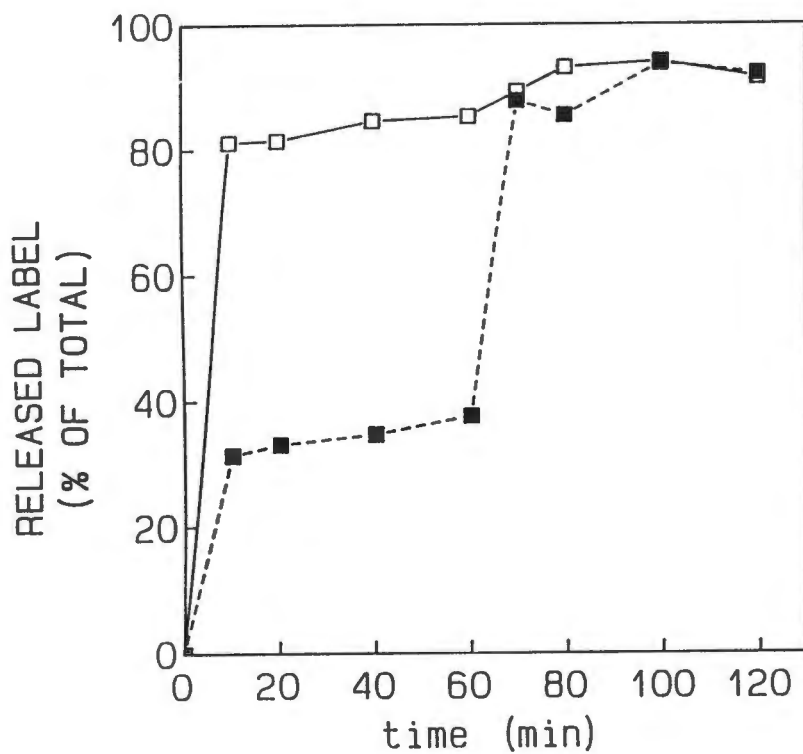
In order to measure internalized label as opposed to cell-surface label, as much remaining surface label had to be removed as was possible. Such removal of surface label is normally achieved by using the enzyme  $\beta$ -galactosidase at 0°C (32), which removes about 85% of the label. This would leave a background surface label of about 15% which is similar to the amount of internalized membrane (14% after 15 minutes. cf. Fig. 9). To see if a greater percentage of surface-bound label could be removed, cells were incubated with proteinase K to proteolytically remove surface proteins and their attached label (Fig.10). Under both isotonic and hypertonic conditions,  $\beta$ -galactosidase removed about 83% of label within 10 minutes at 0°C. This increased to 95% after 2 hours. Proteinase K on the other hand removed only 35% within the first 10 minutes and this increased to about 40% after 60 minutes. Addition of  $\beta$ -galactosidase increased the removal of this label to the same level as with  $\beta$ -galactosidase alone. Proteinase K, therefore, did not help to remove any additional label nor any proteins that may have sterically hindered the action of  $\beta$ -

galactosidase. For further experiments, cell-surface label was removed to about 90% by treatment with  $\beta$ -galactosidase for 30 minutes in the cold.

Molecular-weight distribution of surface-labelled glycoconjugates internalized under hypertonic conditions

To determine the molecular-weight distribution of labelled plasma-membrane glycoconjugates, membrane fractions were analyzed by SDS-PAGE. The profile of internalized surface label analyzed for proteins after internalizing label for 15 minutes at 37°C and removing 90% of the remaining surface label by  $\beta$ -galactosidase treatment prior to membrane preparation, can be seen in figures 11C and 11D, for isotonic and hypertonic conditions respectively.

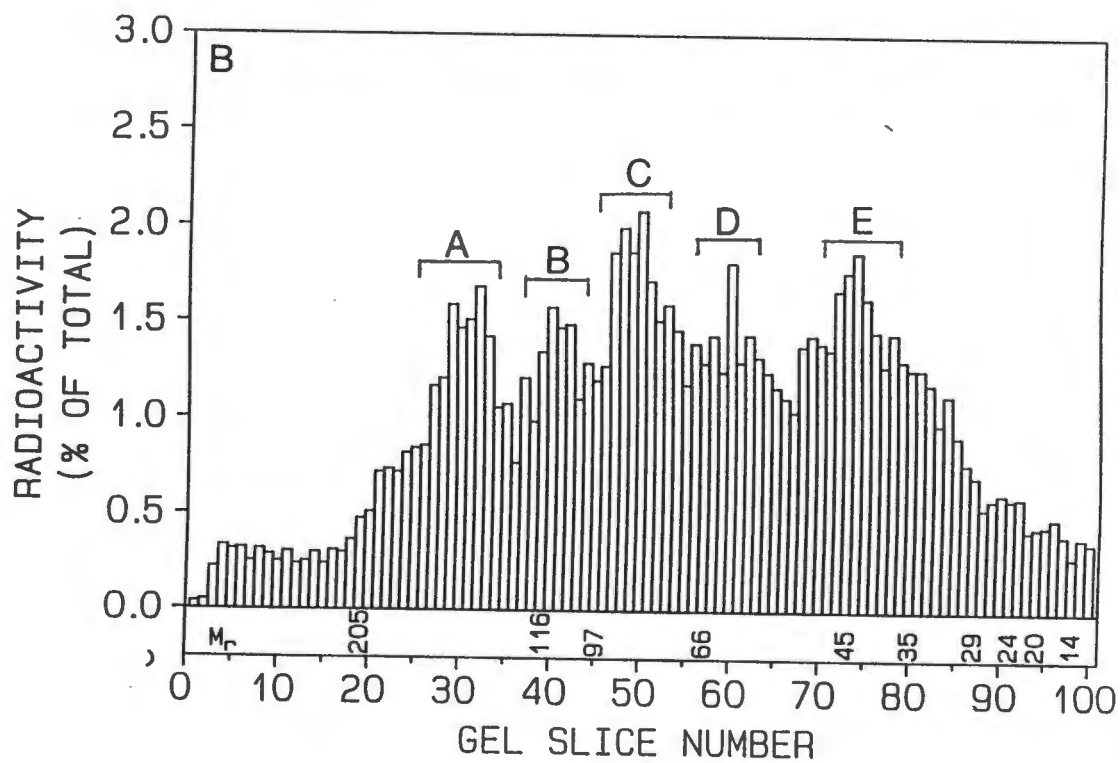
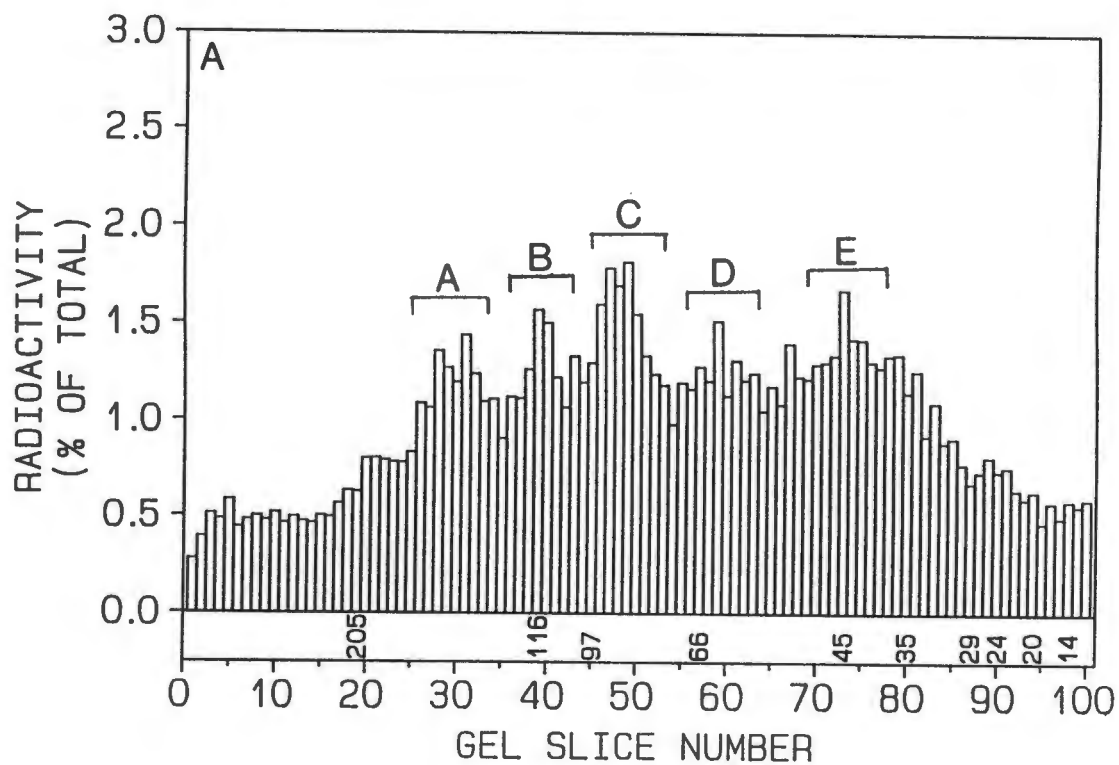
The molecular-weight profile of surface label showed five major peaks, A, B, C, D and E (Fig. 11A and B). These were similar to previous results which indicated slightly more label in peaks A and C relative to the rest (41). This method only resolves classes of proteins of similar mobility rather than specific proteins. Labelling under hypertonic conditions (0.52 osm) did not result in any obvious difference in the species of proteins that became labelled, as judged by the common presence of the five major peaks A, B, C, D and E in both Fig. 11A and 11B. Internalized label (Fig. 11C and 11D) was slightly enriched in molecules of about 90 kD (peak C). Membrane internalization under hypertonic conditions showed the same enrichment and thus no effect of hypertonicity on the components of internalized label could be observed.



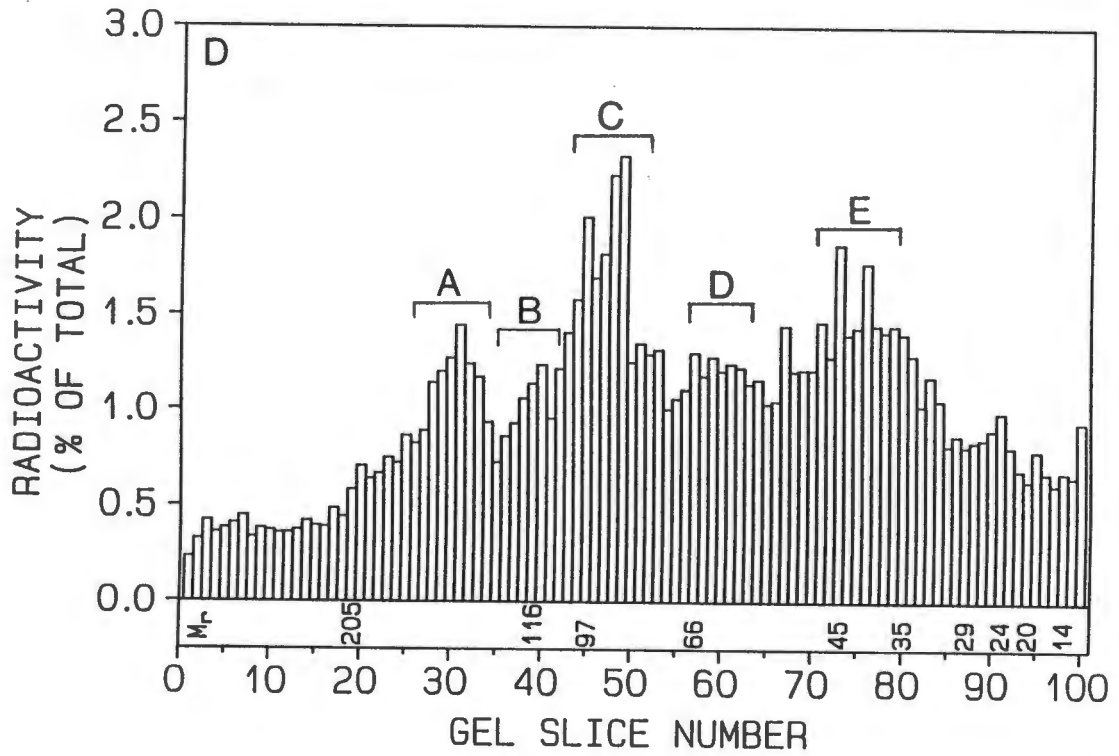
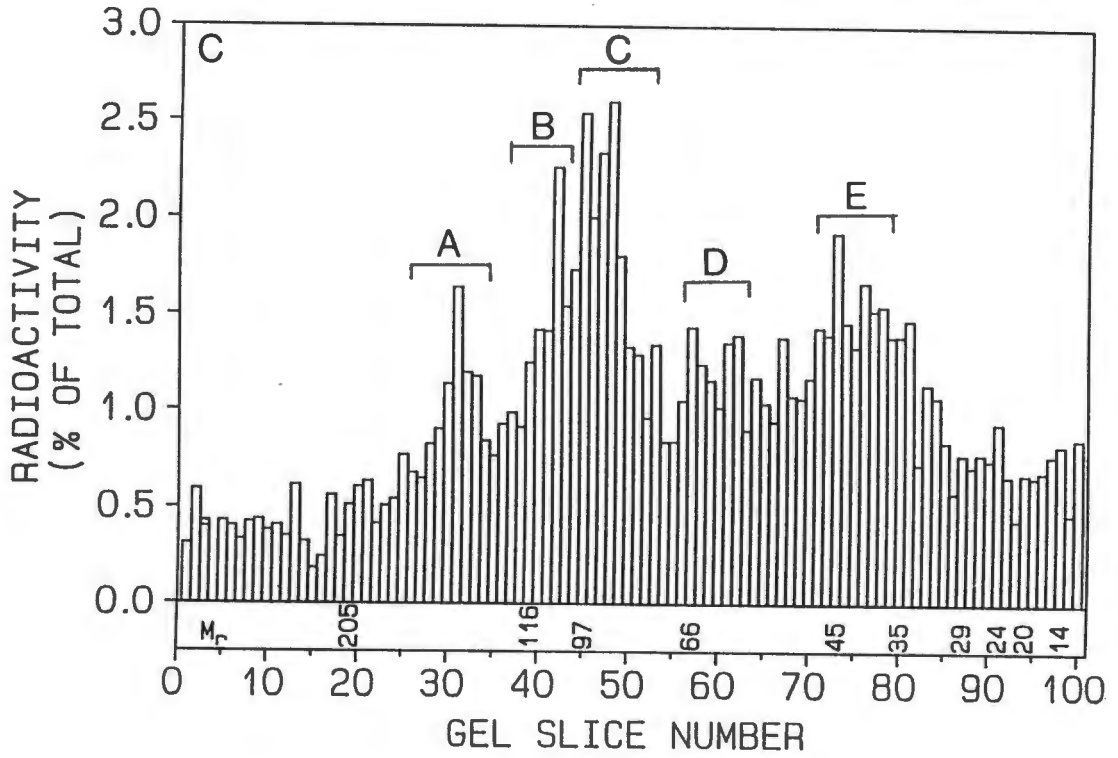
(LEGEND ON FOLLOWING PAGE)

FIG. 10. Kinetics of  $^3\text{H}$ -galactose release from the cell surface under isotonic and hypertonic conditions

Cells were labelled with UDP[6- $^3\text{H}$ ]-galactose, fixed in 2% glutaraldehyde, and washed with 5 volumes of HeRPMI. Cells were then resuspended at  $5 \times 10^7$  cells/ml in 2 ml of either isotonic ( $\square, \blacksquare$ ) or hypertonic ( $\circ, \bullet$ ) medium with  $\beta$ -galactosidase (0.2 units/ml) ( $\square, \circ$ ) or proteinase K (0.5 mg/ml) ( $\blacksquare, \bullet$ ) at 0°C. At the indicated times 200  $\mu\text{l}$  samples of cell suspension were removed, from which 50  $\mu\text{l}$  aliquots were analyzed for either total label or for soluble label remaining in the cell-free supernatant after centrifugation for 30 sec in a microfuge. Radioactivity was measured after conversion to  $^3\text{H}_2\text{O}$  in a sample oxidizer (model 306, Packard Instrument Co.). At the 60 minute time point, proteinase K (0.5 mg/ml) was added to ( $\square, \circ$ ) and  $\beta$ -galactosidase (0.2 units/ml) with PMSF (0.5 mg/ml) was added to ( $\blacksquare, \bullet$ ).



(LEGEND ON PAGE 61)



(LEGEND ON FOLLOWING PAGE)

**FIG. 11. Molecular-weight profile of internalized labelled plasma-membrane glycoconjugates**

Cells were labelled with either UDP[6-<sup>3</sup>H]-galactose (B and D) or UDP[U-<sup>14</sup>C]-galactose (A and C). They were then resuspended in isotonic (A and C) or in hypertonic (B and D) medium and either kept at 4°C for 15 minutes (A and B) to prevent internalization, or incubated at 37°C for 15 minutes (C and D). These were then cooled to 0°C, and treated with β-galactosidase (0.2 units/ml) for 30 minutes. This removed 90% of the surface label. Membranes were then prepared and analyzed on gradient SDS-PAGE. Membranes from A and B were combined, as were membranes from C and D, and applied to the same lanes on the SDS-PAGE. Radioactivity was measured as <sup>3</sup>H<sub>2</sub>O and <sup>14</sup>CO<sub>2</sub> after full separation of the isotopes. Counting accuracy was to ±3% for both <sup>3</sup>H and <sup>14</sup>C.

## CHAPTER 5

### CONCLUSION

The aim of this study was to characterise a compartment of endocytosis-derived membrane traffic, which was not mediated by coated-pit formation. Such a compartment was believed to involve large non-coated vesicles, as coated vesicles have a typical diameter of  $0.1 \mu\text{m}$  and the volume-weighted average diameter of all primary endocytic vesicles was calculated as  $0.24 \mu\text{m}$  (cf. review 20). A population of larger vesicles would thus increase the average size from  $0.1 \mu\text{m}$  to  $0.24 \mu\text{m}$ . In order to measure the size of such proposed larger pinosomes, the contribution of coated vesicles to this average size measurement, would have to be eliminated.

Selective inhibition of coated-pit endocytosis as opposed to fluid-phase endocytosis can be achieved by using hypertonic conditions (34) or by acidification of the cytosol (35) (cf. Table I). Other studies using the above inhibition systems have shown that in the case of fibroblasts both receptor-mediated and fluid-phase endocytosis have been inhibited. The selective effect of hyperosmolarity on endocytosis appears to be cell-type specific (Table I). The effect on endocytosis in P388D1 macrophages was thus determined in this study.

At  $0.52 \text{ osm}$ , fluid-phase uptake kinetics were shown to be markedly biphasic in comparison to the kinetics at isotonicity ( $0.3 \text{ osm}$ ). The initial rate (as measured between 0 and 10 min)

remained unchanged at 0.52 osm but the net uptake rate (measured between 20 and 60 min) was reduced to 52% of the isotonic rate. This was interpreted to mean that 48% of internalized fluid was retroendocytosed. Further increase in osmolarity to 0.63 osm reduced both the initial and the net rate of fluid uptake by 60% relative to the rate at 0.52 osm. Increasing the osmolarity to 0.74 osm had an even greater inhibitory effect on both modes of uptake. The net rate constantly remained at about 50% of the initial rate, above 0.52 osm (Table II). Thus hypertonicity seemed to have a dual effect on fluid-phase uptake. Firstly, it enhanced the retroendocytosis of fluid as determined by net uptake kinetics, and secondly, it had a direct effect on the initial uptake of fluid at higher osmolarities.

The effect of hypertonicity (0.52 osm) on membrane internalization was similar to that on the net uptake of fluid. The rate of internalization ( $k$ ), was slowed to 57.6% of that at isotonicity, with the rates of plasma-membrane uptake being 2.6% and 1.5% per minute for isotonic and hypertonic conditions, respectively. Such a decrease in the internalization rate of labelled glycoconjugates was not due to the exclusion of any particular labelled protein species from the endocytic vesicle (as determined by SDS-PAGE. Fig. 11). There was however a slight enrichment of a protein species of about 90 kD (peak C. Fig. 11C and 11D). This enrichment was found in both isotonic and hypertonic internalized membranes.

TABLE II: The effect of increasing osmolarity on endocytosis (A summary of results)

Osmolarity (Osmoles)	Transferrin Init. rate	Transferrin level	fluid-phase Init. rate	net rate	Internalization rate
0.3	100%	100%	100%	100%	100%
0.52	56.5%	100%	100%	52.2%	57.6%
0.63	26%	63%	40%	18%	-
0.74	22%	46%	32%	13%	-

Initial attempts to use HRP to measure receptor-mediated endocytosis in P388D1 macrophages were promising, when it was found that uptake could be inhibited by 90% at osmolarities above 0.52 osm, but this was found to be due to the inhibition of binding of HRP to the mannose receptor at these high osmolarities. HRP was therefore not suitable for receptor-mediated uptake studies at increased osmolarities.

Transferrin uptake via the transferrin receptor was also inhibited by the hypertonic conditions (Table II). The initial rate of uptake was inhibited by 43.5% at 0.52 osm. The steady-state level (i.e. maximum number of cell-associated transferrin molecules) was not altered at this osmolarity, but, similar to fluid-phase uptake, was affected only above 0.52 osm. Between 0.63 and 0.74 osm increasing osmolarity had the same effect on both initial transferrin uptake and fluid endocytosis (cf. Table II, column 2 vs. column 4). These results suggested that the mechanism of hypertonic inhibition was the same for the two modes of uptake above 0.52 osm, but was different at lower osmolarities.

Selective inhibition of receptor-mediated transferrin endocytosis, as opposed to fluid-phase endocytosis, was achieved at 0.52 osmoles. The initial fluid uptake rate was unaffected at this osmolarity, whereas the rate of transferrin uptake was reduced to 57% of the rate at isotonicity. Despite the fact that the inhibition of transferrin uptake was not complete at 0.52 osm, the result suggested that receptor-mediated endocytosis and fluid-phase uptake involved separate

mechanisms which could be differentially affected by hypertonicity. The extent of inhibition of membrane internalization at 0.52 osm was very similar to that of transferrin uptake at the same osmolarity, and this suggested that receptor-mediated endocytosis is responsible for the majority of bulk plasma-membrane internalization. Such a large contribution to membrane internalization by coated vesicles could be expected, due to their high surface to volume ratio.

The effect of 0.52 osm on the volume-weighted average size of primary pinocytotic vesicles was determined by comparing the initial rate of membrane internalization to the initial rate of fluid-phase uptake. The volume-weighted average size under isotonic conditions was calculated to be 0.66  $\mu\text{m}$  and this increased to 1.15  $\mu\text{m}$  under hypertonic conditions. A size of 0.66  $\mu\text{m}$  was much larger than that calculated previously, as 0.24  $\mu\text{m}$  - 0.28  $\mu\text{m}$ , at isotonicity (32,20). A possible reason for this difference is that the surface area of the cell is larger than previously estimated (cf. Chapter 4). To obtain an isotonic vesicle size of 0.24  $\mu\text{m}$ , the surface area of the cell would have to be 3600  $\mu\text{m}^2$  as opposed to 1300  $\mu\text{m}^2$ . This could be possible as the surface area of another macrophage-like cell-line, J774, has been estimated to be 3900  $\mu\text{m}^2$  (20'). The average size under hypertonic conditions, taking the cell surface area to be 3600  $\mu\text{m}^2$ , was calculated as 0.41  $\mu\text{m}$ . Such a large increase in the average vesicle size (0.24 - 0.41  $\mu\text{m}$ ) with only a 43% inhibition of coated-pit mediated uptake, suggested that these vesicles are very much larger than 0.24  $\mu\text{m}$ . Such large vesicles would be ideal for fluid uptake, as,

due to their low surface to volume ratio, they would be able to include a much greater volume of fluid per unit membrane area than smaller vesicles such as coated vesicles.

The differential effect of hypertonicity between cell types could be due to cell function. Polymorphonuclear leukocytes (34) and the macrophages in the present study are both phagocytic cell types, and both demonstrate selective inhibition of receptor-mediated uptake under hypertonic conditions. Such selective inhibition was not seen in fibroblasts (36,53). Coated pit-mediated endocytosis was shown to be able to incorporate all volume uptake in BHK cells (54), thereby suggesting that no alternative endocytic mechanism existed in this cell type. It is possible that an alternative mechanism involved in fluid-phase uptake exists only in certain cell types, such as phagocytic cells like macrophages and leukocytes. The data presented in this study demonstrate that endocytosis, especially fluid-phase endocytosis, may be more complicated than originally thought.

In order to gain a better understanding of such a possible mechanism, a more detailed analysis of the hypertonic inhibitory effect would be required, both in terms of the osmolarity range used and in terms of the cell type to cell type variation. Such information may indeed illuminate multiple paths of endocytosis involved in specific cell functions.

APPENDIXCalculation of the initial rate of membrane internalization

Membrane internalization values (i.e. % of label on the plasma-membrane) were plotted on a semi-log plot against time, and the half-life estimated directly off the graph. The relative sizes of the plasma-membrane, the first and the second internal compartments with respect to plasma-membrane-derived label, could be determined from the internalization kinetics. These three compartments were labelled  $M_1$ ,  $M_2$  and  $M_3$  respectively (3).

Other parameters used were:

- $r$  = The initial rate of membrane internalization in terms of filling of the first internal compartment.
- $s$  = The relative size of the plasma-membrane with respect to both the plasma-membrane and the first internal compartment ( $M_1/(M_1+M_2)$ ).
- $t_0$  = The turnover time of label in  $M_1$  (i.e. the plasma membrane).
- $k$  = The rate constant for internalizing membrane.

The following data were obtained from the internalization curve.  $M_1 = 0.81$ ;  $M_2 = 0.13$ . Therefore  $s = 0.86$  as calculated by  $0.81/(0.81+0.13)$ .

The rate constant (k) was calculated by solving the following equations:

$$r = \ln 2 / t_{1/2}$$

$$t_0 = [r \cdot (1-s)]^{-1}$$

$$k = M_1 / t_0$$

REFERENCES

1. Davis, C.G., Goldstein, J.L., Südhof, T.C., Anderson, R.G.W., Russell, D.W., and Brown, M.S. (1987) Acid-dependent ligand dissociation and recycling of LDL receptor mediated by growth factor homology region. *Nature* 326 :760-765
2. Harding, C., Heuer, J., and Stahl, P. (1983) Receptor-mediated endocytosis of transferrin and recycling of the transferrin receptor in rat reticulocytes. *J. Cell Biol.* 97 :329-339
3. Geuze, H.J., Slot, J.W., Strous, G.J.A.M., Lodish, H.F., and Schwartz, A.L. (1983) Intracellular site of asialoglycoprotein receptor-ligand uncoupling: Double-label immunoelectron microscopy during receptor-mediated endocytosis. *Cell* 32 : 277-287
4. Dunn, W.A., Connolly, T.P., and Hubbard, A.L. (1986) Receptor-mediated endocytosis of epidermal growth factor by rat hepatocytes: Receptor pathway. *J. Cell Biol.* 102 :24-36
5. Carpentier, J.L., Gorden, P., Robert, A., and Orci, L. (1986) Internalization of polypeptide hormones and receptor recycling. *Experientia* 42 :734-744
6. Brandli, A.W., Parton, R.G., and Simons, K. (1990) Transcytosis in MDCK cells: Identification of glycoproteins transported bidirectionally between both plasma-membrane domains. *J. Cell Biol.* 111 :2909-2921
7. Sandvig, K., and Van Deurs, B. (1990) Selective modulation of the endocytic uptake of ricin and fluid-phase markers without alteration in transferrin endocytosis. *J. Biol. Chem.* 265 :6382-6388
8. Helenius, A., Kartenbeck, J., Simons, K., and Fries, E. (1980) On the entry of semliki forest virus into BHK-21 cell. *J. Cell Biol.* 84 :404-420
9. Anderson, R.G., Goldstein, J.L., and Brown, M.S. (1977) Role of the coated endocytic vesicle in the uptake of receptor-bound low density lipoprotein in human fibroblasts. *Cell* 10 :351-364
10. Bretscher, M.S., Thomson, J.N., and Pearse, B.M.F. (1980) Coated pits act as molecular filters. *Proc. Natl. Acad. Sci. USA* 77 :4156-4159
11. Jing, S., Spencer, T., Miller, K., Hopkins, C., and Trowbridge, I.S. (1990) Role of the human transferrin receptor cytoplasmic domain in endocytosis: Location of a specific signal sequence for internalization. *J. Cell Biol.* 110 :283-294

12. Lazarovits, J., and Roth, M. (1988) A single amino acid change in the cytoplasmic domain allows the influenza virus hemagglutinin to be endocytosed through coated pits. *Cell* 53 :743-752
13. Petersen, O.W., and van Deurs, B. (1983) Serial section analysis of coated pits and vesicles involved in adsorptive pinocytosis in cultured fibroblasts. *J. Cell Biol.* 96 :277-281
14. Yamashiro, D.J., Fluss, S.R., and Maxfield, F.R. (1983) Acidification of endocytic vesicles by an ATP dependent proton pump. *J. Cell Biol.* 97 :929-934
15. Geuze, H.J., Slot, J.W., and Schwartz, A.L. (1987) Membranes of sorting organelles display lateral heterogeneity in receptor distribution. *J. Cell Biol.* 104 :1715-1723
16. Geuze, H.J., Slot, J.W., Strous, G.J.A.M., and Schwartz, A.L. (1983) The pathway of asialoglycoprotein-ligand during receptor-mediated endocytosis: A morphological study with colloidal gold/ligand in the human hepatoma cell-line Hep G2. *Eur. J. Cell Biol.* 32 :38-44
17. Anderson, R.G.W., Brown, M.S., Beisiegel, U., and Goldstein, J.L. (1982) Surface distribution and recycling of the Low Density Lipoprotein receptor as visualized with antireceptor antibodies. *J. Cell Biol.* 93 :523-521
18. Brown, W.J., and Farquhar, M.G. (1984) Accumulation of coated vesicles bearing mannose-6-phosphate receptors for lysosomal enzymes in the Golgi region of I-cell fibroblasts. *Proc. Natl. Acad. Sci. USA* 81 :5135-5139
19. Carpentier, J.L., Gorden, P., Anderson, R.G.W., Goldstein, J.L., Brown, M.S., Cohen, S., and Orci, L. (1982) Co-localization of <sup>125</sup>I-epidermal growth factor and ferritin-low density lipoprotein in coated pits: A quantitative electron microscopic study in normal and mutant human fibroblasts. *J. Cell Biol.* 95 :73-77
20. Thilo, L. (1985) Quantification of endocytosis-derived membrane traffic. *Biochim. Biophys. Acta* 822 :243-266
21. Klausner, R.D., Van Renswoude, J., Ashwell, G., Kempf, C., Schechter, A.N., Dean, A., and Bridges, K.R. (1983) Receptor-mediated endocytosis of transferrin in K562 cells. *J. Biol. Chem.* 258 :4715-4724
22. Thilo, L., and Burgert, H-G. (1983) Monensin does not prevent recycling of plasma-membrane glycoconjugates. *Exp. Cell Res.* 147 :297-302

23. Casey, K.A., Maurey, K.M., and Storrie, B. (1986) Characterization of early compartments in fluid-phase pinocytosis: a cell fractionation study. *J. Cell Sci.* 83 :119-133
24. Steinman, R.M., Brodie, S.E., and Cohn, Z.A. (1976) Membrane flow during pinocytosis: A serologic analysis. *J. Cell Biol.* 68 :665-687
25. McKinley, D.N., and Wiley, H.S. (1988) Reassessment of fluid-phase endocytosis and diacytosis in monolayer cultures of human fibroblasts. *J. Cell. Physiol.* 136 :389-397
26. Scharschmidt, B.F., Lake, J.R., Renner, E.L., Licko, V., and Van Dyke, R.W. (1986) Fluid-phase endocytosis by cultured rat hepatocytes and perfused rat liver: Implication for plasma-membrane turnover and vesicular trafficking of fluid-phase markers. *Proc. Natl. Acad. Sci. USA* 83 :9488-9492
27. England, I.G., Naess, L., Blomhoff, R., and Berg, T. (1986) Uptake, intracellular transport and release of  $^{125}\text{I}$ -polyvinylpyrrolidone and [ $^{14}\text{C}$ ]-sucrose-asialofetuin in rat liver parenchymal cells. *Biochem. Pharmacol.* 35 :201-208
28. Besterman, J.M., Airhart, J.A., Woodworth, R.C., and Low, R.B. (1981) Exocytosis of pinocytosed fluid in cultured cells: Kinetic evidence for rapid turnover and compartmentation. *J. Cell Biol.* 91 :716-727
29. Lowry, O.H., Rosebrough, N.J., Farr, A.L., and Randall, R.J. (1951) Protein measurement with the folin phenol reagent. *J. Biol. Chem.* 193 :265-275
30. Ose, L., Ose, T., Reinertsen, R., and Berg, T. (1980) Fluid endocytosis in isolated rat parenchymal and non-parenchymal liver cells. *Exp. Cell Res.* 126 :109-119
31. Steinman, R.M., Mellman, I.S., Muller, W.A., and Cohn, Z.A. (1983) Endocytosis and recycling of plasma membrane. *J. Cell Biol.* 96 :1-27
32. Burgert, H-G., and Thilo, L. (1983) Internalization and recycling of plasma-membrane glycoconjugates during pinocytosis in the macrophage cell-line P388D1. *Exp. Cell Res.* 144 :127-142
33. de Chastelier, C., Lang, T., Ryter, A., and Thilo, L. (1987) Exchange kinetics and composition of endocytic membranes in terms of plasma-membrane constituents: A morphometric study in macrophages. *Eur. J. Cell Biol.* 44 :112-123

34. Daukas, G., and Zigmond, S.H. (1985) Inhibition of receptor-mediated but not fluid-phase endocytosis in polymorphonuclear leukocytes. *J. Cell Biol.* 101 :1673-1679
35. Sandvig, K., Olsnes, S., Petersen, O.W., and van Deurs, B. (1987) Acidification of the cytosol inhibits endocytosis from coated pits. *J. Cell Biol.* 105 :679-689
36. Heuser, J.E., and Anderson, R.G.W. (1989) Hypertonic media inhibit receptor-mediated endocytosis by blocking clathrin-coated pit formation. *J. Cell Biol.* 108 :389-400
37. Heuser, J. (1989) Effects of cytoplasmic acidification on clathrin lattice morphology. *J. Cell Biol.* 108 :401-411
38. Koren, H.S., Handwerger, B.S., and Wunderlich, J.R. (1975) Identification of macrophage-like characteristics in a cultured mouse tumour line. *J. Immunol.* 114 :894
39. Snyderman, R., Pike, M.C., Fischer, D.G., and Koren, H.S. (1977) Biologic and biochemical activities of continuous macrophage cell-lines P388D1 and J774.1. *J. Immunol.* 119 :2060
40. Oliver, J.M., Berlin, R.D., and Davis, B.H. (1984) Use of horseradish peroxidase and fluorescent dextrans to study fluid-phase pinocytosis in leukocytes. *Methods in Enzymol.* 108 :336-347
41. Haylett, T., and Thilo, L. (1986) Limited and selective transfer of plasma-membrane glycoproteins to membrane of secondary lysosomes. *J. Cell Biol.* 103 :1249-1256
42. Thilo, L. (1983) Labelling of plasma-membrane glycoconjugates by terminal galactosylation (galactosyltransferase and glycosidase). *Methods in Enzymol.* 98 :415-421
43. Heigler, H.T., Maxfield, F.R., Willingham, M.C., and Pastan, I. (1980) Dansylcadaverine inhibits internalization of <sup>125</sup>I-Epidermal growth factor in BALB 3T3 cells. *J. Biol. Chem.* 255 :1239-1241
44. Fraker, P.J., and Speck, J. (1978) Protein and cell membrane iodinations with a sparingly soluble chloroamide, 1,3,4,6-tetrachloro-3a,6a-diphenylglycouril. *Biochem. Biophys. Res. Commun.* 80 :849-857
45. Karin, M., and Mintz, B. (1981) Receptor-mediated endocytosis of transferrin in developmentally totipotent mouse teratocarcinoma stem cells. *J. Biol. Chem.* 256 :3245-3252
46. Bar-Sagi, D., and Feramisco, J.R. (1986) Induction of membrane ruffling and fluid-phase pinocytosis in quiescent fibroblasts by ras proteins. *Science* 233 :1061-1068

47. Lang, T., and de Chastelier, C. (1985) Fluid-phase and mannose receptor-mediated uptake of horseradish peroxidase in mouse bone marrow-derived macrophages: Biochemical and ultrastructural study. *Biol. Cell* 53 :149-154
48. Sung, S.J., Nelson, R.S., and Silverstein, S.C. (1983) The role of the mannose/N-Acetylglucosamine receptor in the pinocytosis of horseradish peroxidase by mouse peritoneal macrophages. *J. Cell. Physiol.* 16 :21-25
49. Stahl, P.D., and Schlesinger, P.H. (1980) Receptor-mediated pinocytosis of mannose/N-Acetylglucosamine terminated glycoproteins and lysosomal enzymes by macrophages. *Trends in Biochem. Sci.* 5 :194
50. Stahl, P.D., Schlesinger, P.H., Sigardson, E., Rodman, J.S., and Lee, Y.C. (1980) Receptor-mediated pinocytosis of mannose glycoconjugates by macrophages: Characterization and evidence for receptor recycling. *Cell* 19 :207-215
51. Oka, J.A., and Weigel, P.H. (1988) Effects of hyperosmolarity on ligand processing and receptor recycling in the hepatic galactosyl receptor system. *J. Cell. Physiol.* 36 :169-183
52. Oka, J.A., Christensen, M.D., and Weigel, P.H. (1989) Hyperosmolarity inhibits galactosyl receptor-mediated but not fluid-phase endocytosis in isolated rat hepatocytes. *J. Biol. Chem.* 264 :12016-12024
53. Carpentier, J.L., Sawano, F., Geiger, D., Gorden, P., Perrelet, A., and Orci, L. (1989) Potassium depletion and hypertonic medium reduce "non-coated" and clathrin-coated pit formation, as well as endocytosis through these two gates. *J. Cell. Physiol.* 138 :519-526
54. Marsh, M., and Helenius, A. (1980) Adsorptive endocytosis of semliki forest virus. *J. Mol. Biol.* 142 :439-454
55. Goldstein, J.L., Brown, M.S., Anderson, R.G.W., Russell, D.W., and Schneider, W.J. (1985) Receptor-mediated endocytosis. *Ann. Rev. Cell. Biol.* 1 :1-39
56. Hopkins, C.R., and Trowbridge, I.S. (1983) Internalization and processing of transferrin and the transferrin receptor in human carcinoma A431 cells. *J. Cell Biol.* 97 :508-521
57. van Renswoude, J., Bridges, K.R., Harford, J.B.L., and Klausner, R.D. (1982) Receptor-mediated endocytosis of transferrin and the uptake of Fe in K562 cells: Identification of a non-lysosomal acidic compartment. *Proc. Natl. Acad. Sci. USA* 79 :6186-6190

58. Dautry-Varsat, A., Ciechanover, A., and Lodish, H.F. (1983) pH and the recycling of transferrin during receptor-mediated endocytosis. *Proc. Natl. Acad. Sci. USA* 80 :2258-2262
59. Ciechanover, A., Schwartz, A.L., Dautry-Varsat, A., and Lodish, H.F. (1983) Kinetics of internalization and recycling of transferrin and the transferrin receptor in a human hepatoma cell-line. *J. Biol. Chem.* 258 :9681-9689
60. Mellman, I.S., Steinman, R.M., Unkeless, J.C., and Cohn, Z.A. (1980) Selective iodination and polypeptide composition of pinocytotic vesicles. *J. Cell Biol.* 86 :712-722
61. Edge, S.B., Hoeg, J.M., Triche, T., Schneider, P.D., and Brewer, H.B. (1986) Cultured human hepatocytes: Evidence for metabolism of low density lipoproteins by a pathway independent of the classical low density lipoprotein receptor. *J. Biol. Chem.* 261 :3800-3806
62. Oka, J.A., and Weigel, P.H. (1983) Recycling of the asialoglycoprotein receptor in isolated rat hepatocytes. *J. Biol. Chem.* 258 :10253-10262
63. Weigel, P.H., Clarke, B.L., and Oka, J.A. (1986) The hepatic galactosyl receptor system: Two different ligand dissociation pathways are mediated by distinct receptor populations. *Biochem. Biophys. Res. Commun.* 140 :43-50
64. Stahl, P., and Gordon, S. (1982) Expression of mannosyl-fucosyl receptor for endocytosis on cultured primary macrophages and their hybrids. *J. Cell Biol.* 93 :49-56
65. Cosson, P., de Curtis, I., Pouyssegur, J., Griffiths, G., and Davoust, J. (1989) Low cytoplasmic pH inhibits endocytosis and transport from the trans-Golgi network to the cell surface. *J. Cell Biol.* 108 :377-387
66. Larkin, J.M., Brown, M.S., Goldstein, J.L., and Anderson, R.G.W. (1983) Depletion of intracellular potassium arrests coated pit formation and receptor-mediated endocytosis in fibroblasts. *Cell* 33 :273-285
67. Davoust, J., Gruenberg, J., and Howell, K.E. (1987) Two threshold values of low pH block endocytosis at different stages. *EMBO J.* 6 :3601-3609